ORGANOMETALLICS

Article

pubs.acs.org/Organometallics

Terms of Use

Synthesis and Characterization of Hydrido Carbonyl Molybdenum and Tungsten PNP Pincer Complexes

Özgür Öztopcu,[†] Christian Holzhacker,[†] Michael Puchberger,[‡] Matthias Weil,[§] Kurt Mereiter,[§] Luis F. Veiros,[∥] and Karl Kirchner*,[†]

[†]Institute of Applied Synthetic Chemistry, [‡]Institute of Materials Chemistry, and [§]Institute of Chemical Technologies and Analytics, Vienna University of Technology, Getreidemarkt 9, A-1060 Vienna, Austria

[∥]Centro de Química Estrutural, Instituto Superior Técnico, Universidade Técnica de Lisboa, Av. Rovisco Pais No. 1, 1049-001 Lisboa, Portugal

Supporting Information

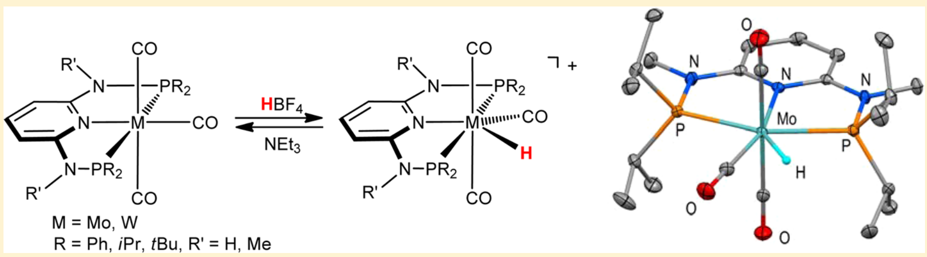

ABSTRACT: In the present study the Mo(0) and W(0) complexes $[M(PNP)(CO)_3]$ as well as seven-coordinate cationic hydridocarbonyl Mo(II) and W(II) complexes of the type $[M(PNP)(CO)_3H]^+$, featuring PNP pincer ligands based on 2,6-diaminopyridine, have been prepared and fully characterized. The synthesis of Mo(0) complexes $[Mo(PNP)(CO)_3]$ was accomplished by treatment of $[Mo(CO)_3(CH_3CN)_3]$ with the respective PNP ligands. The analogous W(0) complexes were prepared by reduction of the bromocarbonyl complexes $[W(PNP)(CO)_3Br]^+$ with NaHg. These intermediates were obtained from the known dinuclear complex $[W(CO)_4(\mu\text{-Br})Br]_2$, prepared in situ from $W(CO)_6$ and stoichiometric amounts of Br_2. Addition of HBF_4 to $[M(PNP)(CO)_3]$ resulted in clean protonation at the molybdenum and tungsten centers to generate the Mo(II) and W(II) hydride complexes $[M(PNP)(CO)_3H]^+$. The protonation is fully reversible, and upon addition of NEt_3 as base the Mo(0) and W(0) complexes $[M(PNP)(CO)_3]$ are regenerated quantitatively. All heptacoordinate complexes exhibit fluxional behavior in solution. The mechanism of the dynamic process of the hydrido carbonyl complexes was investigated by means of DFT calculations, revealing that it occurs in a single step. The structures of representative complexes were determined by X-ray single-crystal analyses.

INTRODUCTION

Tridentate PNP ligands in which the central pyridine-based ring donor contains $-CH_2PR_2$ substituents in the two ortho positions are widely utilized ligands in transition-metal chemistry (e.g., Fe, Ru, Rh, Ir, Pd, Pt).[1−10] As part of our effort to create tridentate PNP pincer-type ligands in which the steric, electronic, and stereochemical properties can be easily varied, we have recently described the synthesis of a series of modularly designed PNP ligands based on N-heterocyclic diamines and R_2PCl which contain both bulky and electron-rich dialkylphosphines as well as various P−O bond containing achiral and chiral phosphine units.[11] In these PNP ligands the central pyridine ring contains $-NR'PR_2$ (R′ = H, alkyl, R = alkyl, aryl) substituents in the two ortho positions. This methodology was first developed for the synthesis of *N,N′*-bis(diphenylphosphino)-2,6-diaminopyridine (PNP-Ph).[12]

With these types of PNP ligands, we have thus far studied their reactivity toward different transition-metal fragments, which resulted in the preparation of a range of new pincer transition-metal complexes, including several new square-planar Ni(II), Pd(II), and Pt(II) PNP complexes,[13] various iron complexes acting as CO sensors[14] and catalysts for the coupling of aromatic aldehydes with ethyldiazoacetate,[15] and several pentacoordinated nickel complexes.[16] Surprisingly, as far as group 6 PNP complexes are concerned, only a few examples have been described in the literature. A few years ago Haupt and co-workers reported the synthesis of $[M(PNP\text{-}Ph)(CO)_3]$ (M = Cr, Mo, W),[12] while Walton and co-workers described the synthesis of the dinuclear molybdenum complex $[Mo(PNP)Mo(HPCy_2)Cl_3]$ (PNP = 2,6-bis-(dicyclohexylphosphinomethyl)pyridine).[17] Most recently, dinuclear molybdenum and tungsten dinitrogen complexes bearing bulky PNP pincer ligands were found to work as effective catalysts for the formation of ammonia from dinitrogen.[18] Finally, Templeton and co-workers described the synthesis of a series of hydrido carbonyl and halo carbonyl tungsten pincer complexes featuring the silazane-based PNP

Received: March 25, 2013
Published: May 7, 2013

pincer-type ligand $HN(SiMe_2CH_2PPh_2)_2$.[19] In a preliminary study we have prepared cationic seven-coordinate halo carbonyl molybdenum pincer complexes of the types $[Mo(PNP\text{-}i\text{Pr})(CO)_3I]^+$ and $[Mo(PNP\text{-}i\text{Pr})(CO)_2(CH_3CN)I]^+$.[13] Here we report on the synthesis, characterization, and reactivity of a series of new hydrido carbonyl molybdenum(II) and tungsten(II) PNP pincer complexes.[20]

■ RESULTS AND DISCUSSION

Molybdenum(0) and Tungsten(0) Complexes. We have recently reported the synthesis of molybdenum tricarbonyl complexes of the type $[Mo(PNP)(CO)_3]$ (**2a−c**) by reacting $[Mo(CO)_3(CH_3CN)_3]$, prepared in situ by refluxing a solution of $[Mo(CO)_6]$ in CH_3CN for 4 h, with the PNP ligands PNP-Ph (**1a**), PNP-*i*Pr (**1b**), and PNP-*t*Bu (**1c**) in 74−90% isolated yields.[13] The same procedure was followed with the N-methylated PNP ligand PNP^{Me}-*i*Pr (**1d**), affording $[Mo(PNP^{Me}\text{-}i\text{Pr})(CO)_3]$ (**2d**) in 80% yield (Scheme 1). The new

Scheme 1

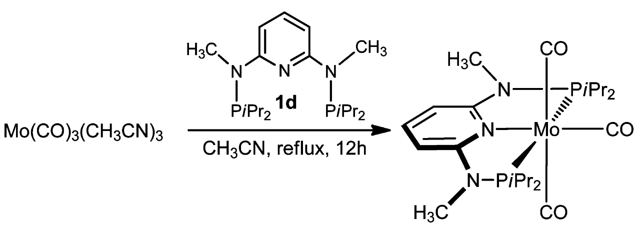

2d PNP^{Me}-*i*Pr

PNP ligand **1d** was prepared in a three-step procedure involving borane protection of the phosphine, a deprotonation/alkylation step, and deprotection of the phosphine, as shown in Scheme 2. The analogous tungsten complexes

Scheme 2

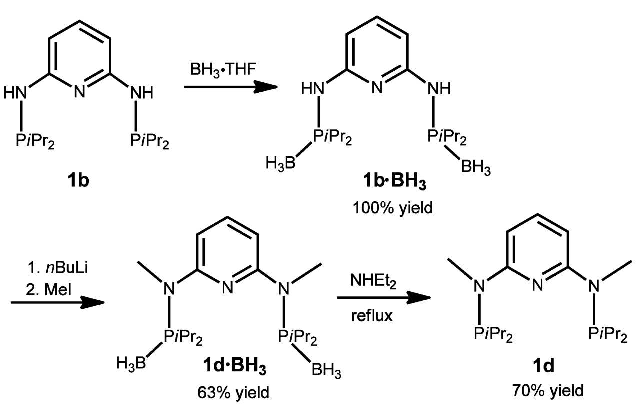

$[W(PNP)(CO)_3]$ can be prepared in a similar fashion but require much longer reaction times (several days to prepare the intermediate $[W(CO)_3(CH_3CN)_3]$); moreover, the yields turned out to be significantly lower (10−25%). It has to be noted that already a few years ago Haupt and co-workers reported the synthesis of $[M(PNP\text{-}Ph)(CO_3)]$ (M = Mo, W) in 34 and 22% yields.[12] We thus developed an alternative method to obtain tungsten(0) complexes $[W(PNP)(CO)_3]$ via the intermediacy of the known dinuclear complex $[W(CO)_4(\mu\text{-}Br)Br]_2$,[21] prepared in situ from $W(CO)_6$ and stoichiometric amounts of Br_2 in CH_2Cl_2 at −70 °C. Treatment of a solution of $[W(CO)_4(\mu\text{-}Br)Br]_2$ in CH_2Cl_2 at room temperature with the PNP ligands **1a−c** afforded on workup the seven-coordinate tungsten(II) complexes $[W(PNP)(CO)_3Br]Br$ (**3a−c**) in 60−80% yields (Scheme 3).

It has to be noted that the reaction of PNP ligands with $[Mo(CO)_4(\mu\text{-}Br)Br]_2$,[21] prepared in situ from $Mo(CO)_6$ and Br_2 in CH_2Cl_2 at −70 °C, affords the analogous seven-coordinate molybdenum complexes $[Mo(PNP)(CO)_3Br]Br$. This has been demonstrated for the synthesis of $[Mo(PNP\text{-}Ph)(CO)_3Br]Br$ (**4a**) and $[Mo(PNP\text{-}i\text{Pr})(CO)_3Br]Br$ (**4b**), as illustrated in Scheme 3.

The solid-state structures of **3a** and **4b** were determined by single-crystal X-ray diffraction. Molecular views of **3a** and **4b** are depicted in Figures 1 and 2, respectively, with selected bond distances and angles reported in the captions. While the Mo-bonded bromide in **4b** was clearly in an axial position, the bromide in the tungsten complex **3a** adopted an axial position at about 86% occupancy (Br1 in Figure 1), while the remaining 14% exchanged places with the carbonyl group C32−O3.

Stirring complexes **3a−c** with an excess of 10% sodium amalgam in THF gave the desired W(0) complexes $[W(PNP\text{-}Ph)(CO)_3]$ (**5a**), $[W(PNP\text{-}i\text{Pr})(CO)_3]$ (**5b**), and $[W(PNP\text{-}t\text{Bu})(CO)_3]$ (**5c**) as yellow solids in 70−80% isolated yields (Scheme 3). This methodology also yields the analogous Mo(0) complexesl thus being an alternative method to that described previously.[13] The use of Zn as reducing reagent turned out to be problematic, due to the formation of highly soluble and, thus, difficult to remove bromozincate anions, e.g., $[ZnBr_3\cdot\text{solvent}]^-$ (solvent = acetone, THF) and $ZnBr_4^{2-}$. Complexes **5a−c** were fully characterized by a combination of ^1H, $^{13}C\{^1H\}$, and $^{31}P\{^1H\}$ NMR spectroscopy, IR spectroscopy, and elemental analysis. Characteristic features of **5a−c** comprise, in the $^{13}C\{^1H\}$ NMR spectrum, two low-field triplet resonances (1/2 ratio) in the ranges of 206−221 and 196−210 ppm assignable to the carbonyl carbon atoms *trans* and *cis* to the pyridine nitrogen, respectively. The $^{31}P\{^1H\}$ NMR spectra exhibit singlet resonances at 85.2, 106.6.1, and 131.6 ppm with $^1J_{WP}$ coupling constants of 315−329 Hz. The tungsten−phosphorus coupling was observed as a doublet satellite due to ^{183}W, 14% abundance with $I = {}^1/_2$, superimposed over the dominant singlet. The IR spectra show the typical three strong to medium absorption bands of a *mer* CO arrangement in the range of 2017−1760 cm^{-1} assignable to one weaker symmetric and two strong asymmetric ν_{CO} stretching modes. The ν_{CO} frequencies, in particular the symmetric CO stretch, is indicative of the increasing electron donor strengths of the PNP ligands and follow the order PNP-Ph < PNP-*i*Pr ≈ PNP^{Me}-*i*Pr < PNP-*t*Bu (Table 1). The CO stretching frequencies are 1964 (**2a**, PNP-Ph), 1936 (**2b**, PNP-*i*Pr), 1936 (**2d**, PNP^{Me}-*i*Pr), and 1922 cm^{-1} (**2c**, PNP-*t*Bu). The same order is found for the respective tungsten complexes. In all complexes the PNP pincer ligand adopts the typical *mer* coordination mode with no evidence for any *fac* isomers.[22]

In addition to the spectroscopic characterization, the solid-state structures of **2d** and **5b,c** were determined by single-crystal X-ray diffraction. Structural views are depicted in Figures 3−5, respectively, with selected bond distances and angles given in the captions. The coordination geometry around the tungsten center of **5b,c** corresponds to a distorted octahedron with P1−W−P2 and *trans*-C_{CO}−W−C_{CO} bond angles 154.43(4) and 165.7(2)° (**5b**), and 151.42(1) and 156.46(9)° (**5c**), respectively. For comparison, in the analogous

Scheme 3

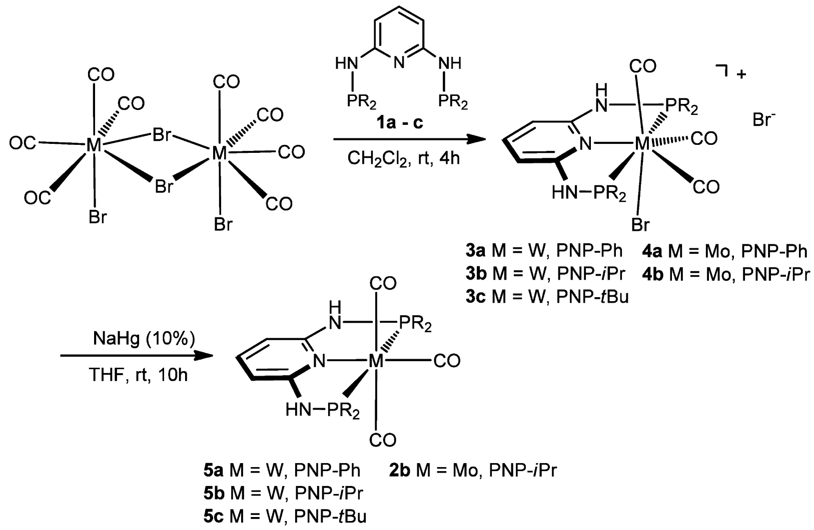

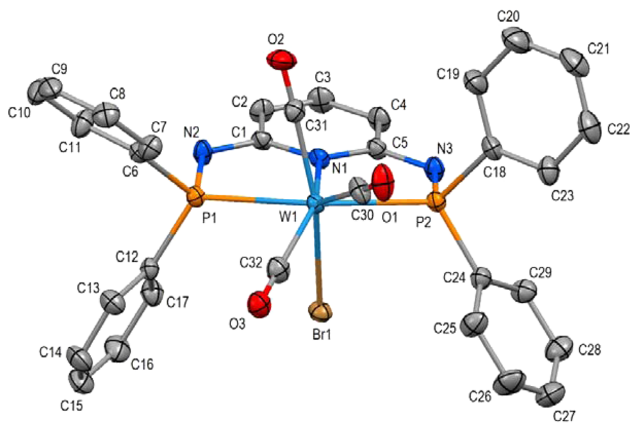

Figure 1. Structural view of [W(PNP-Ph)$(CO)_3$Br]Br·CH_3OH (**3a**·CH_3OH) showing 20% thermal ellipsoids (H atoms, Br^- counterion, solvent molecule and subordinate Br/CO positions omitted for clarity). Selected bond lengths (Å) and bond angles (deg): W−C(31) = 2.017(5), W−C(30) = 2.020(6), W−C(32) = 2.024(8), W−N(1) = 2.237(3), W−P(1) = 2.4955(10), W−P(2) = 2.4895(11), W−Br(1) = 2.6015(5); P(1)−W−P(2) = 152.34(4), N(1)−W−P(1) = 77.44(9), N(1)−W−P(2) = 75.92(9), N(1)−W−C(30) = 137.76(16), N(1)−W−C(31) = 82.35(16), N(1)−W−C(32) = 150.87(8), N(1)−W−Br(1) = 82.28(9).

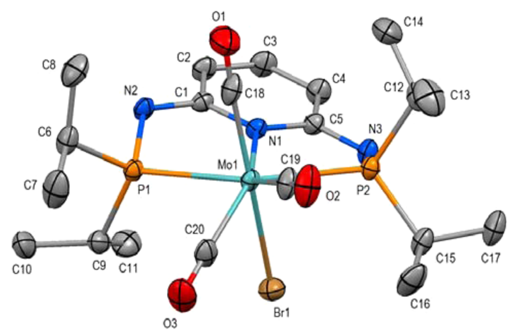

Figure 2. Structural view of [Mo(PNP-*i*Pr)$(CO)_3$Br]Br (**4b**) showing 50% thermal ellipsoids (Br^- counterion omitted for clarity). Selected bond lengths (Å) and bond angles (deg): Mo−C(18) = 2.037(2), Mo−C(19) = 1.979(2), Mo−C(20) = 2.006(2), Mo−N(1) = 2.236(2), Mo−P(1) = 2.5242(5), Mo−P(2) = 2.5172(5), Mo−Br(1) = 2.6713(3); P(1)−Mo−P(2) = 150.80(2), N(1)−Mo−P(1) = 75.67(4), N(1)−Mo−P(2) = 75.35(4), N(1)−Mo−C(18) = 85.95(7), N(1)−Mo−C(19) = 77.73(6), N(1)−Mo−C(20) = 127.23(6), N(1)−Mo−Br(1) = 84.22(4).

[Mo(PNP)$(CO)_3$] complexes **2a−d** the P1−Mo−P2 angles are hardly affected by the size of the substituents of the phosphorus atoms, being 155.0(2), 155.62(1), 155.3(1), and 151.73(1)°, respectively.[12,13] The carbonyl−Mo−carbonyl angles of the CO ligands *trans* to one another, on the other hand, vary strongly with the bulkiness of the PR_2 moiety (PNP-Ph_2 < PNP-*i*Pr_2 < PNP^{Me}-*i*Pr < PNP-*t*Bu_2) and decrease from 171.1(8)° in [Mo(PNP-Ph)$(CO)_3$], to 166.03(5)° in [Mo(PNP-*i*Pr)$(CO)_3$], to 162.93(7)° in [Mo(PNP^{Me}-*i*Pr)$(CO)_3$], and finally to 156.53(4)° in [Mo(PNP-*t*Bu)$(CO)_3$].

Molybdenum(II) and Tungsten(II) Hydride Complexes. Addition of HBF_4 to a CH_2Cl_2 solution of [Mo(PNP)$(CO)_3$] (**2a−d**) and [W(PNP)$(CO)_3$] (**5a−c**) resulted in an immediate color change from yellow to pale yellow consistent with protonation at the tungsten and molybdenum centers to generate tungsten(II) and molybdenum(II) hydride complexes [Mo(PNP)$(CO)_3$H]BF_4 (**7a−d**) and [W(PNP)$(CO)_3$H]BF_4 (**8a−c**), respectively (Scheme 4). The protonation is fully reversible, and upon addition of NEt_3 as base the Mo(0) and W(0) complexes [M(PNP)$(CO)_3$] are re-formed

Table 1. Selected IR, $^{31}P\{^1H\}$ NMR, and $^{13}C\{^1H\}$ NMR Data for [M(PNP)$(CO)_3$] and [M(PNP)$(CO)_3$H]$^+$ (M = Mo, W)

complex	ν_{CO}, cm^{-1}	δ_P, ppm	δ_{CO}, ppm	δ_H, ppm
2a	1964, 1858, 1765	116.2	228.4, 211.2	
2b	1936, 1809, 1790	143.6	231.4, 216.9	
2c	1922, 1808, 1771	161.9	233.1, 224.0	
2d	1936, 1810, 1795	171.0	230.8, 217.9	
5a	1955, 1847, 1759	100.2	206.0, 196.6	
5b	1929, 1805, 1784	128.5	221.1, 210.6	
5c	1914, 1799, 1759	147.2	224.7, 219.4	
7a	2042, 1940, 1937	111.5, 97.8	212.7, 203.2	−3.78
7b	2035, 1923, 1920	142.3, 121.4	212.3, 205.8	−4.98
7c	2019, 1937, 1916	158.8, 142.8	213.7, 209.5	−4.34
7d	2028, 1928, 1910	166.1, 147.7	210.8, 205.4	−5.49
8a	2038, 1963, 1918	95.5, 84.8	205.9, 196.6	−3.43
8b	2027, 1910, 1906	125.9, 108.6	205.5, 198.0	−4.83
8c	2021, 1934, 1897	141.1, 126.8		−4.16

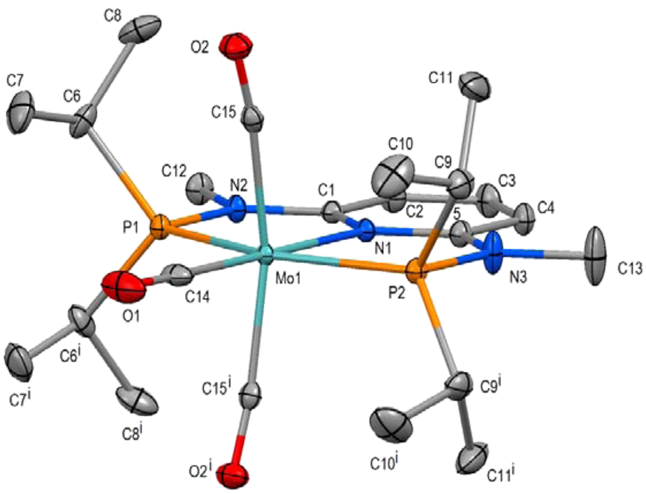

Figure 3. Structural view of $[Mo(PNP^{Me}\text{-}i\text{Pr})(CO)_3]$ (**2d**) showing 50% thermal ellipsoids (H atoms are omitted for clarity; the complex is mirror symmetric; symmetry code i for x, $^1/_2 - y$, z). Selected bond lengths (Å) and bond angles (deg): Mo–C(14) = 1.956(2), Mo–C(15) = 2.0153(13), Mo–N(1) = 2.2589(15), Mo–P(1) = 2.3977(5), Mo–P(2) = 2.4070(5); P(1)–Mo–P(2) = 155.25(2), N(1)–Mo–P(1) = 77.74(4), N(1)–Mo–P(2) = 77.51(4), N(1)–Mo–C(15) = 98.52(4), C(15)–Mo–C(15^i) = 162.93(7).

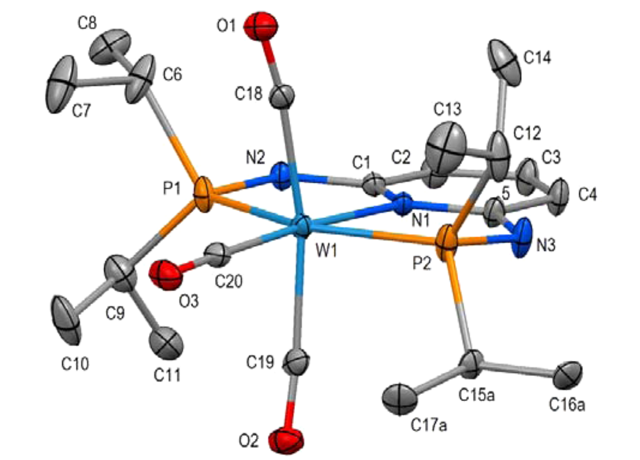

Figure 4. Structural view of $[W(PNP\text{-}i\text{Pr})(CO)_3]\cdot THF\cdot{}^1/_2C_6H_{14}$ (**5b**$\cdot THF\cdot{}^1/_2C_6H_{14}$) showing 30% thermal ellipsoids (H atoms, solvent molecules, and alternative orientation of *i*Pr group C(16a)–C(15a)–C(17a) omitted for clarity). Selected bond lengths (Å) and bond angles (deg): W–C(18) = 2.014(5), W–C(19) = 2.015(5), W–C(20) = 1.934(4), W–N(1) = 2.257(3), W–P(1) = 2.4080(12), W–P(2) = 2.4013(12); P(1)–W–P(2) = 154.43(4), N(1)–W–P(1) = 77.30(9), N(1)–W–P(2) = 77.18(9), N(1)–W–C(18) = 100.8(2), N(1)–W–C(19) = 93.3(2), N(1)–W–C(20) = 175.8(2), C(18)–W–C(19) = 165.7(2).

quantitatively (Scheme 4). All hydride complexes are thermally robust pale yellow solids that are air stable in the solid state but slowly decompose in solution. Characterization was accomplished by elemental analysis and by ^{1}H, ^{13}C{^{1}H}, and ^{31}P{^{1}H} NMR and IR spectroscopy (Table 1). The recording of a ^{13}C{^{1}H} NMR spectrum of **8c** was precluded due to the poor solubility of this complex in most common solvents.

Seven-coordinate complexes are well-known for their fluxional behavior in solution,[23,24] since typically none of the idealized geometries such as capped prism, capped octahedron, and pentagonal bipyramid or any of the less symmetrical

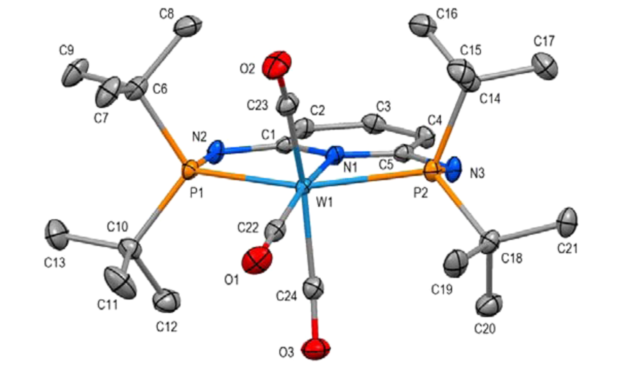

Figure 5. Structural view of $[W(PNP\text{-}t\text{Bu})(CO)_3]\cdot THF$ (**5c**$\cdot$THF) showing 50% thermal ellipsoids (H atoms and solvent molecule omitted for clarity). Selected bond lengths (Å) and bond angles (deg): W–C(22) = 1.941(3), W–C(23) = 1.997(2), W–C(24) = 2.001(2), W–N(1) = 2.277(2), W–P(1) = 2.4583(5), W–P(2) = 2.4656(5); P(1)–W–P(2) = 151.42(2), N(1)–W–P(1) = 76.52(4), N(1)–W–P(2) = 76.00(4), N(1)–W–C(22) = 169.53(8), N(1)–W–C(23) = 113.16(8), N(1)–W–C(24) = 90.27(7), C(23)–W–C(24) = 156.46(9).

Scheme 4

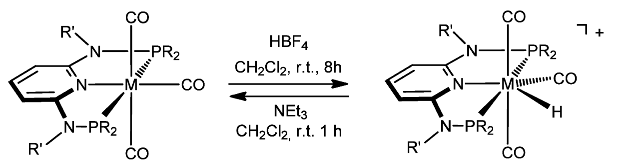

2a-d M = Mo
5a-c M = W

7a M = Mo, PNP-Ph
7b M = Mo, PNP-*i*Pr
7c M = Mo, PNP-*t*Bu
7d M = Mo, PNP^{Me}-*i*Pr
8a M = W, PNP-Ph
8b M = W, PNP-*i*Pr
8c M = W, PNP-*t*Bu

arrangements are typically characterized by a markedly lower total energy.[25] Hence, interconversions between these various structures are quite facile. The fluxional behavior of complexes **7a–d** and **8a–c** was evident in variable-temperature ^{1}H and ^{31}P{^{1}H} NMR spectra. At room temperature, the ^{1}H NMR spectrum of complexes **7** and **8** confirmed the presence of one hydride ligand, which appeared in the range of −3.89 to −5.36 ppm either as a well-resolved doublet of doublets (**8b**,**c**) or as triplets (**7a–d**, **8a**).

At −60 °C, all hydride resonances appear as a well-resolved doublet of doublets with one large and one small coupling constant of about 21–36 and 47–53 Hz, respectively. As an example, the variable-temperature 300 MHz ^{1}H NMR spectra of the hydride region of $[Mo(PNP\text{-}Ph)(CO)_3H]BF_4$ (**7a**) are shown in Figure 6. At low temperatures the hydride signal constitutes the X part of an AMX spin system, giving rise to a doublet of doublets which, at elevated temperatures in the fast exchange regime, becomes a simple A_2X spin system where the X part exhibits a triplet resonance.

In the ^{13}C{^{1}H} NMR spectrum of complexes **7a–d** and **8a–d** the most noticeable resonances are two low-field resonances of the carbonyl carbon atoms *trans* and *cis* to the pyridine nitrogen observed as two triplets in a 1:2 ratio. At room temperature, no ^{31}P{^{1}H} NMR signals could be detected for molybdenum complexes **7a–d** and the tungsten complex **8a** due to their fluxional behavior. At −60 °C, however, the ^{31}P{^{1}H} NMR spectra of all complexes **8** give rise to two doublets with a large geminal coupling constant of about 80 Hz, which is indicative of the phosphorus atoms being in mutually *trans* positions. The IR spectra of **7** and **8** show three strong to

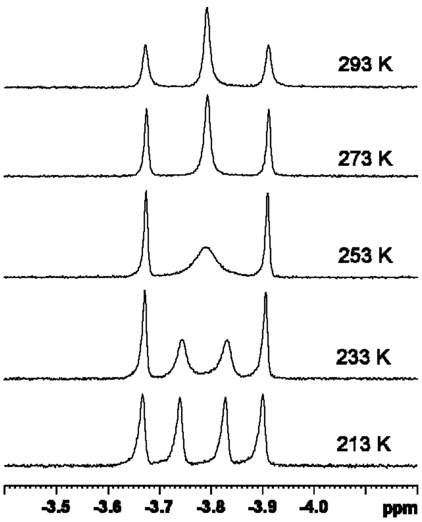

Figure 6. Variable-temperature 300 MHz ^{1}H NMR spectra of the hydride region of [Mo(PNP-Ph)(CO)$_3$H]BF$_4$ (**7a**) in CD_2Cl_2.

medium absorption ν_{CO} bands of the one symmetric and the two asymmetric vibration modes (Table 1), which again are typical for a *mer* CO arrangement.

In addition to the spectroscopic characterization, the solid-state structures of **7a**,**d** and **8a** were determined by single-crystal X-ray diffraction. Structural diagrams are depicted in Figures 7–9, respectively, with selected bond distances given in the captions. The coordination geometry around the molybdenum center corresponds to a distorted capped octahedron, in which a hydride ligand occupies the capping position of an octahedral face. The crystal structure showed the tridentate PNP ligand to be bound meridionally with three carbonyl ligands filling the remaining three sites. The carbonyl *trans* to nitrogen was pushed toward one of the phosphine ligands to accommodate the hydride ligand. The metal–hydride bond length in the three complexes averages 1.65 Å (1.64–1.70 Å), the mean bond angle H–M–P to the nearest P atom is 67° (65–69°), and the mean bond angle H–M–C between hydride and the equatorial carbonyl group is 53° (50–55°). The hydride to carbonyl C atom distance (1.62 Å in **7d**) and the almost linear attachment of the equatorial carbonyl group (Mo1–C22–O3 = 179° in **7d**) do not indicate a significant bonding interaction between hydride and the adjacent carbonyl C atom in the three structurally characterized hydrido carbonyl complexes.

The mechanism of the dynamic process of the hydrido carbonyl complexes was investigated by means of DFT

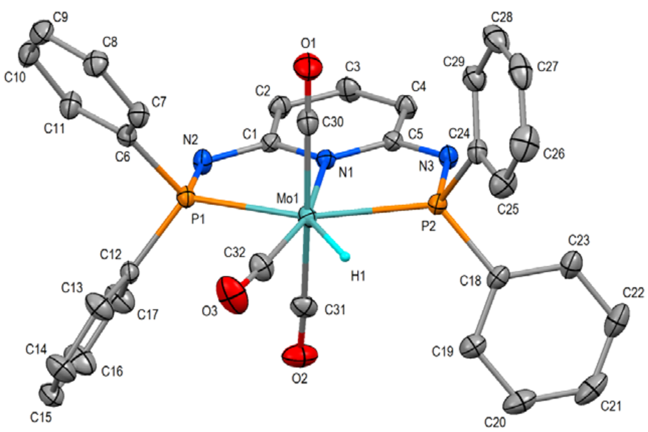

Figure 7. Structural view of [Mo(PNP-Ph)(CO)$_3$H]BF$_4$ (**7a**) showing 50% thermal ellipsoids (BF_4^- counterion and alternative orientation of C(32)–O(3) and H(1) omitted for clarity). Selected bond lengths (Å) and bond angles (deg): Mo–H(1) = 1.67(4), Mo–C(30) = 2.0368(15), Mo–C(31) = 2.0465(15), Mo–C(32) = 2.017(3), Mo–N(1) = 2.2357(11), Mo–P(1) = 2.4409(4), Mo–P(2) = 2.4489(4); P(1)–Mo–P(2) = 154.64(1), N(1)–Mo–P(1) = 77.39(3), N(1)–Mo–P(2) = 77.39(3), N(1)–Mo–C(30) = 87.62(5), N(1)–Mo–C(31) = 86.97(5), N(1)–Mo–C(32) = 163.73(9), N(1)–Mo–H(1) = 146.0(15), C(32)–Mo–H(1) = 50.2(15).

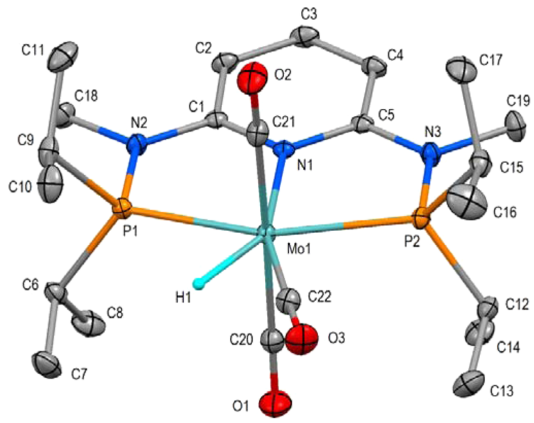

Figure 8. Structural view of [Mo(PNP^{Me}-*i*Pr)(CO)$_3$H]BF$_4$·CH_2Cl_2 (**7d**·CH_2Cl_2) showing 50% thermal ellipsoids (BF_4^- counterion and CH_2Cl_2 omitted for clarity). Selected bond lengths (Å) and bond angles (deg): Mo–H(1) = 1.63(2), Mo–C(20) = 2.0440(13), Mo–C(21) = 2.0239(13), Mo–C(22) = 1.9856(13), Mo–N(1) = 2.2462(10), Mo–P(1) = 2.4425(3), Mo–P(2) = 2.4776(3); P(1)–Mo–P(2) = 154.61(1), N(1)–Mo–P(1) = 77.29(3), N(1)–Mo–P(2) = 77.31(3), N(1)–Mo–C(20) = 94.27(4), N(1)–Mo–C(21) = 89.76(4), N(1)–Mo–C(22) = 162.26(4), N(1)–Mo–H(1) = 145.7(8), C(22)–Mo–H(1) = 52.0(8).

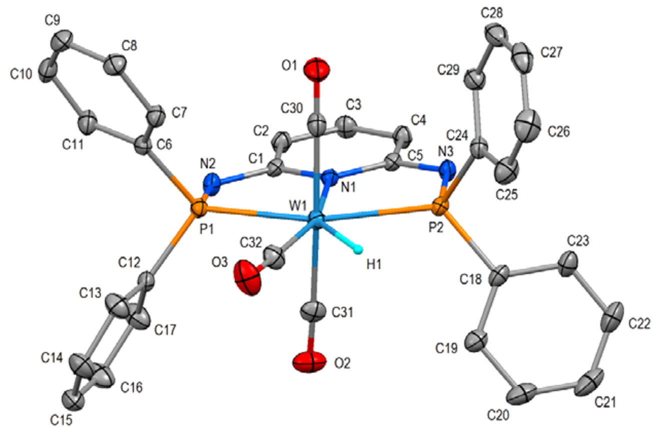

Figure 9. Structural view of [W(PNP-Ph)(CO)$_3$H]BF$_4$ (**8a**) showing 50% thermal ellipsoids (BF_4^- counterion and alternative orientation of C(32)–O(3) and H(1) omitted for clarity). Selected bond lengths (Å) and bond angles (deg): W–H(1) = 1.65(5), W–C(30) = 2.033(2), W–C(31) = 2.039(2), W–C(32) = 2.022(4), W–N(1) = 2.2316(15), W–P(1) = 2.4444(5), W–P(2) = 2.4459(5); P(1)–W–P(2) = 154.32(2), N(1)–W–P(1) = 77.17(4), N(1)–W–P(2) = 77.29(4), N(1)–W–C(30) = 87.78(7), N(1)–W–C(31) = 86.88(7), N(1)–W–C(32) = 162.35(11), N(1)–W–H(1) = 143.5(17), C(32)–W–H(1) = 53.9(17).

calculations[26] for the molybdenum and tungsten complexes $[Mo(PNP)(CO)_3H]^+$ (**7a–c**) and $[W(PNP)(CO)_3H]^+$ (**8a–c**). The free energy profile for the "pseudorotation" is depicted in Figure 10. The optimized structures of **8a,c** and the corresponding transition states **TS** are shown in Figures 11 and 12. In the fluxional process, the CO and the hydride ligands in the PNP plane exchange positions in a single-step path. During that process the rest of the molecule has to change in order to accommodate the overall transformations associated with the pseudorotation. The main geometry change that happens along the path is the hydride ligand moving from the PNP plane to the perpendicular plane, i.e., the plane of the three CO ligands, in the transition state (**TS**) and then back to the PNP plane again but on the other side of the CO ligand. Thus, in **TS**, the two *trans* CO ligands have to create enough space to allow the presence of an extra ligand in the NCCC plane, opening the corresponding OC–M–CO angle and bending away from the hydride ligand. Accordingly, In the case of the molybdenum and tungsten PNP complexes bearing the less bulky Ph and iPr substituents (**7a,b** and **8a,b**), the C30–W1–C31 angle changes from about 177° in the ground-state structure to 166° in **TS**, where both *trans* CO ligands are bent toward the PNP ligand (Figure 11). On the other hand, in the case of the molybdenum and tungsten PNP complexes bearing the bulky *t*Bu substituents (**7c** and **8c**) the situation is somewhat different. The C30–W1–C31 angle increases from 169° in the minima to 178° in **TS**, while one of the two *trans* CO ligands is severely bent away from the PNP ligand and the other one is bent toward the PNP ligand (Figure 12). In the course of all these transformations also the H1–W1–C32 angles change from about 55° in **7a–c** and **8a–c** to roughly 43° in the **TS**, respectively. Bond distances are hardly affected by the interconversion. It is interesting to note that, in agreement with the X-ray structures of **7a**, **7d**, and **8a** (Figures 6–8), the distance between H1 and C32 is rather short, being in the range of 1.80–1.66 Å. A Wiberg index[27] of 0.20, in **8c**, seems to indicate an attractive interaction between the hydride and the neighboring C_{CO} atom (C32). Most importantly, the free energy barriers $\Delta G^{\ddagger}$ are 18.6 and 21.3 kcal/mol for **7c** and **8c**, respectively, containing the bulky *t*Bu substituents. In the case of all other complexes the free energy barrier is lower, being in the range of 12.5–16.1 kcal/mol, as shown in Figure 9. These results corroborate a process that can be stopped in the temperature range employed in the NMR studies and a more facile process in the case of the Mo species, as observed.

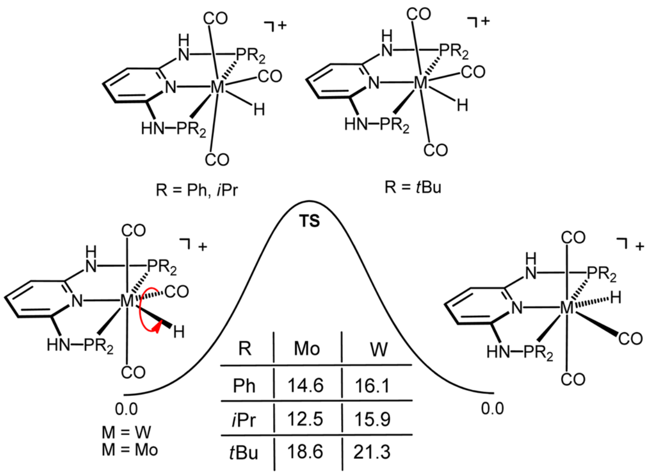

R	Mo	W
Ph	14.6	16.1
*i*Pr	12.5	15.9
*t*Bu	18.6	21.3

Figure 10. Free energy profile (in kcal/mol) for the "pseudorotation" of CO and hydride ligands in the complexes $[M(PNP)(CO)_3H]^+$ (M = W, Mo).

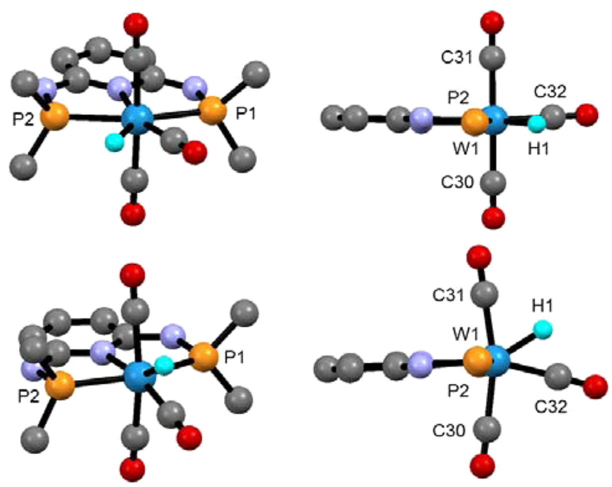

Figure 11. Front (left) and side views (right) of the optimized structures (DFT/B3LYP) of the tungsten complex $[W(PNP\text{-}Ph)(CO)_3H]^+$ (**8a**; top) and the transition state **TS** (bottom) with most phenyl carbon atoms and hydrogen atoms omitted for clarity.

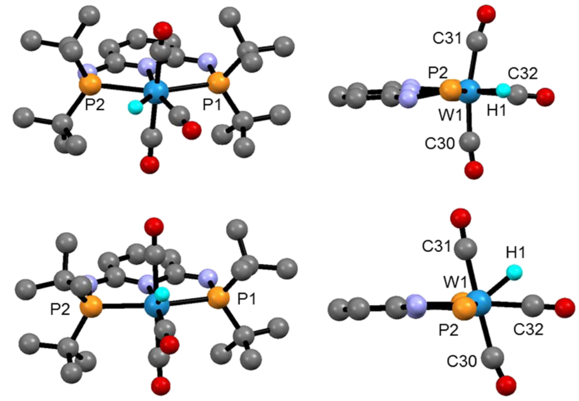

Figure 12. Front (left) and side views (right) of the optimized structures (DFT/B3LYP) of the tungsten complex $[W(PNP\text{-}tBu)(CO)_3H]^+$ (**8c**; top) and the transition state **TS** (bottom) with most *t*Bu carbon atoms and hydrogen atoms omitted for clarity.

■ CONCLUSION

In the present study the Mo(0) and W(0) complexes $[M(PNP)CO)_3]$ as well as seven-coordinate cationic hydrido carbonyl and halo carbonyl Mo(II) and W(II) complexes of the type $[M(PNP)(CO)_3Br]^+$ and $[M(PNP)(CO)_3H]^+$ featuring PNP pincer ligands based on 2,6-diaminopyridine were prepared and fully characterized. The synthesis of the Mo(0) complexes $[Mo(PNP)CO)_3]$ was accomplished by treatment of $[Mo(CO)_3(CH_3CN)_3]$ with the respective PNP ligands. The analogous W(0) complexes were prepared by reduction of the bromo carbonyl complexes $[W(PNP)(CO)_3Br]^+$ with NaHg. These intermediates were obtained from the known dinuclear complex $[W(CO)_4(\mu\text{-Br})Br]_2$, prepared in situ from $W(CO)_6$ and stoichiometric amounts of Br_2. Addition of HBF_4 to $[M(PNP)(CO)_3]$ resulted in protonation at the tungsten and molybdenum centers to formally generate the Mo(II) and W(II) hydride complexes $[M(PNP)(CO)_3H]^+$. The protonation is fully reversible, and upon addition of NEt_3 as base the Mo(0) and W(0) complexes $[M(PNP)(CO)_3]$ are re-formed quantitatively. All seven-coordinate complexes exhibit fluxional behavior in solution, since none of the idealized geometries (capped prism, capped octahedron, and pentagonal bipyramid) or any of the less symmetrical arrangements are typically characterized by a markedly lower total energy. The mechanism of the dynamic process of the hydrido carbonyl complexes was investigated by means of DFT calculations, revealing that it occurs in a single step. Thereby the CO and the hydride ligands which are situated in the PNP plane are interconverted. The structures of representative complexes were determined by X-ray single-crystal analyses.

■ EXPERIMENTAL SECTION

General Considerations. All manipulations were performed under an inert atmosphere of argon by using Schlenk techniques. The solvents were purified according to standard procedures.[28] The ligands and complexes *N,N′*-bis(diphenylphosphino)-2,6-diaminopyridine (PNP-Ph; **1a**), N,N′-bis(diisopropylphosphino)-2,6-diaminopyridine (PNP-*i*Pr; **1b**), *N,N′*-bis(di-*tert*-butylphosphino)-2,6-diaminopyridine (PNP-*t*Bu; **1c**), [Mo(PNP-Ph)$(CO)_3$] (**2a**), [Mo(PNP-*i*Pr)$(CO)_3$] (**2b**), and [Mo(PNP-*t*Bu)$(CO)_3$] (**2c**) were prepared according to the literature.[13] The deuterated solvents were purchased from Aldrich and dried over 4 Å molecular sieves. ^{1}H, ^{13}C{^{1}H}, and ^{31}P{^{1}H} NMR spectra were recorded on Bruker AVANCE-250 and AVANCE-300 DPX spectrometers and were referenced to $SiMe_4$ and H_3PO_4 (85%), respectively.

***N,N′*-Bis(diisopropylphosphino-borane)-2,6-diaminopyridine (PNP-*i*Pr; 1b·BH$_3$).** BH_3·THF (43.1 mL, 1.0 M, 43.06 mmol) was added slowly to a solution of **1b** (7.00 g, 20.50 mmol) in 100 mL of dry THF. After the mixture was stirred for 30 min at room temperature, the solvent was evaporated under reduced pressure. The white solid was further dried under vacuum for 2 h to give the product in quantitative yield. Anal. Calcd for $C_{17}H_{39}B_2N_3P_2$: C, 55.32; H, 10.65; N, 11.39. Found: C, 55.28; H, 10.70; N, 11.43. ^{1}H NMR (δ, $CDCl_3$, 20 °C): 7.32 (t, J = 7.9 Hz, 1H, py^4), 6.26 (d, J = 7.9, 2H, py^{3,5}), 4.58 (d, J = 8.4 Hz, 2H, N*H*), 2.62 (septd, J = 6.9 Hz, J = 13.7 Hz, 4H, C*H*$(CH_3)_2$), 1.16 (m, 24H, CH(C*H*$_3$)$_2$), 0.60 to −0.15 (bs, 6H, B*H*$_3$). ^{13}C{^{1}H} NMR (δ, $CDCl_3$, 20 °C): 154.4 (s, py^{2,6}), 140.1 (s, py^4), 103.1 (s, py^{3,5}), 24.5 (d, J = 36.3 Hz, $CH(CH_3)_2$), 17.2 (d, J = 4.3 Hz, $CH(CH_3)_2$), 17.0 (s, $CH(CH_3)_2$). ^{31}P{^{1}H} NMR (δ, $CDCl_3$, 20 °C): 88.5 (br, m).

***N,N′*-Bis(diisopropylphosphino-borane)-*N,N′*-methyl-2,6-diaminopyridine (PNP^{Me}-*i*Pr; 1d·BH$_3$).** To a solution of **1b·BH$_3$** (7.45 g, 20.19 mmol) in THF (50 mL) at −20 °C was slowly added *n*-BuLi (17.0 mL, 2.5 M, 41.39 mmol). The reaction mixture was allowed to reach room temperature and was stirred for 2 h. Methyl iodide (3.15 mL, 50.46 mmol) was then added slowly via syringe. After the mixture was stirred for 12 h at room temperature, the reaction was quenched with a saturated NH_4Cl solution (100 mL) and 5 mL of concentrated NH_3. The aqueous phase was extracted twice with CH_2Cl_2, and the combined organic phases were washed with 25 mL of brine and dried over Na_2SO_4. The solvent was removed under reduced pressure to afford **1d·BH$_3$** as a yellow oil. The crude product was purified via flash chromatography using silica gel and THF to give the product as a white solid. Anal. Calcd for $C_{19}H_{43}B_2N_3P_2$: C, 57.56; H, 10.91; N, 10.58. Found: C, 57.62; H, 10.89; N, 10.61. Yield: 5.05 g (63%). ^{1}H NMR (δ, $CDCl_3$, 20 °C): 7.48 (t, J = 8.0 Hz, 1H, py^4), 6.49 (d, J = 8.0, 2H, py^{3,5}), 3.17 (d, J = 7.9 Hz, 6H, NC*H*$_3$), 2.80 (septd, J = 7.0 Hz, J = 21.2 Hz, 4H, C*H*$(CH_3)_2$), 1.22 (dd, J_1 = 6.9 Hz, J_2 = 16.5 Hz, 12H, CH(C*H*$_3$)$_2$), 1.03 (dd, J = 7.0 Hz, J = 15.11 Hz, 12H, CH(C*H*$_3$)$_2$), 0.70 to −0.30 (bs, 6H, B*H*$_3$). ^{13}C{^{1}H} NMR (δ, $CDCl_3$, 20 °C): 156.9 (s, py^{2,6}), 139.1 (s, py^4), 105.8 (s, py^{3,5}), 37.6 (s, NCH_3), 25.6 (d, J = 36.2 Hz, $CH(CH_3)_2$), 17.8 (s, $CH(CH_3)_2$), 17.2 (s, $CH(CH_3)_2$). ^{31}P{^{1}H} NMR (δ, $CDCl_3$, 20 °C): 105.9 (br, m).

***N,N′*-Bis(diisopropylphosphino)-*N,N′*-methyl-2,6-diaminopyridine (PNP^{Me}-*i*Pr; 1d).** **1d·BH$_3$** (5.00 g, 12.59 mmol) was refluxed for 72 h in 100 mL of Et_2NH. After removal of the solvent under reduced pressure the remaining oil was dissolved in THF, filtered through Celite, and obtained as a yellow oil after evaportaion of the solvent under reduced pressure. The crude product was purified by recrystallization from acetonitrile to afford **2d** as a white solid. Anal. Calcd for $C_{19}H_{37}N_3P_2$: C, 61.77; H, 10.09; N, 11.37. Found: C, 61.69; H, 10.16; N, 11.44. Yield: 3.25 g (70%). ^{1}H NMR (δ, CD_2Cl_2, 20 °C): 7.22 (t, J = 8.0 Hz, 1H, py^4), 6.64 (bs, py^{3,5}), 3.04 (d, J = 2.3 Hz, 6H, NC*H*$_3$), 2.22 (bs, 4H, C*H*$(CH_3)_2$), 1.10 (dd, J = 6.9 Hz, J = 16.9 Hz, 12H, CH(C*H*$_3$)$_2$), 0.98 (dd, J = 7.0 Hz, J = 12.1 Hz, 12H, CH(C*H*$_3$)$_2$). ^{13}C{^{1}H} NMR (δ, CD_2Cl_2, 20 °C): 160.4 (s, py^{2,6}), 136.9 (s, py^4), 99.1 (d, J = 22.3 Hz, py^{3,5}), 33.7 (bs, NCH_3), 26.2 (d, J = 15.3 Hz, $CH(CH_3)_2$), 19.4 (s, $CH(CH_3)_2$), 19.2 (s, $CH(CH_3)_2$), 19.0 (s, $CH(CH_3)_2$). ^{31}P{^{1}H} NMR (δ, CD_2Cl_2, 20 °C): 81.3 (bs).

[Mo(PNP^{Me}-*i*Pr)(CO)$_3$] (2d). A suspension of $Mo(CO)_6$ (714 mg 2.7 mmol) in acetonitrile (10 mL) was refluxed for 4 h. After that PNP^{Me}-*i*Pr (**1d**; 1.00 g, 2.7 mmol) was added and the mixture was refluxed for an additional 12 h. The solvent was then removed under reduced pressure, and the product was washed twice with diethyl ether and dried under vacuum. Yield: 1.19 g (80%). Anal. Calcd for $C_{22}H_{37}MoN_3O_3P_2$: C, 48.09; H, 6.79; N, 7.65. Found: C, 48.15; H, 6.82; N, 7.61. ^{1}H NMR (δ, CD_2Cl_2, 20 °C): 7.40 (t, J = 7.6 Hz, 1H, py), 6.30 (d, J = 7.6 Hz, 2H, py), 3.01 (s, 6H, NC*H*$_3$), 2.47 (m, 4H, C*H*$(CH_3)_2$), 1.30 (m, 12H, CH(C*H*$_3$)$_2$), 1.09 (m, 12H, CH(C*H*$_3$)$_2$). ^{13}C{^{1}H} NMR (δ, CD_2Cl_2, 20 °C): 230.8 (t, J = 6.0 Hz, CO), 217.9 (t, J = 10.8 Hz, CO), 174.9 (t, J = 2.6 Hz, py), 137.8 (s, py), 96.7 (t, J = 2.2 Hz, py), 33.9 (t, J = 1.8 Hz, $N(CH_3)_2$), 32.9 (t, J = 9.0 Hz, $CH(CH_3)_2$), 29.6 (s, $N(CH_3)_2$), 19.2 (t, J = 7.5 Hz, $CH(CH_3)_2$), 18.1 (s, $CH(CH_3)_2$). ^{31}P{^{1}H} NMR (δ, CD_2Cl_2, 20 °C): 171.0 (s). IR (ATR, cm^{-1}): 1936 (ν_{CO}), 1810 (ν_{CO}), 1795 (ν_{CO}).

[W(PNP-Ph)(CO)$_3$Br]Br (3a). To a suspension of $W(CO)_6$ (2.0 g, 5.68 mmol) in CH_2Cl_2 (30 mL) was added Br_2 (292 μL, 5.68 mmol) at −70 °C, and the mixture was stirred for 1 h at that temperature and for an additional 1 h at room temperature. After that, PNP-Ph (**1a**; 2.72 g, 5.68 mmol) was added and the mixture was stirred for 5 h at room temperature. After removal of the solvent under reduced pressure, a yellow solid was obtained, which was washed with a 1/9 methanol/diethyl ether mixture and dried under vacuum. Yield: 4.11 g (80%). Anal. Calcd for $C_{32}H_{25}Br_2N_3O_3P_2W$: C, 42.46; H, 2.78; N, 4.64. Found: C, 42.29; H, 2.79; N, 4.55. ^{1}H NMR (δ, acetone-d_6, 20 °C): 10.85 (bs, 2H, N*H*), 7.78 (bs, 11H, py, Ph), 7.60 (bs, 10H, Ph), 7.43 (d, J = 7.6 Hz, 2H, py). ^{13}C{^{1}H} NMR (δ, $CDCl_3$, 20 °C): 225.4 (t, J = 10.3 Hz, CO), 210.3 (t, J = 8.6 Hz, CO), 159.7 (d, J = 7.5 Hz, py), 159.6 (d, J = 7.5 Hz, py), 133.1 (s, py), 131.9 (s, Ph), 131.9 (s, Ph), 129.0 (d, J = 5.0 Hz, Ph), 128.2 (d, J = 5.4 Hz, Ph), 103.1 (s, py). ^{31}P{^{1}H} NMR (δ, acetone-d_6, 20 °C): 85.2. IR (ATR, cm^{-1}): 2030 (ν_{CO}), 1958 (ν_{CO}), 1933 (ν_{CO}).

[W(PNP-*i*Pr)(CO)$_3$Br]Br (3b). This complex was prepared analogously to **3a** with $W(CO)_6$ (2.0 g, 5.68 mmol) and PNP-*i*Pr (**1b**; 1.95 g, 5.69 mmol) as starting materials. Yield: 3.06 g (70%). Anal. Calcd for $C_{20}H_{33}Br_2N_3O_3P_2W$: C, 31.23; H, 4.32; N, 5.46. Found: C, 31.13; H, 4.42; N, 5.50. ^{1}H NMR (δ, CD_2Cl_2, 20 °C): 9.32 (bs, 2H, N*H*), 7.66 (t, J = 7.2 Hz, 1H, py), 6.67 (d, J = 8.1 Hz, 2H, py), 3.54 (m, 2H, C*H*$(CH_3)_2$), 2.88 (m, 2H, C*H*$(CH_3)_2$), 1.43 (m, 24H, CH(C*H*$_3$)$_2$). ^{13}C{^{1}H} NMR (δ, CD_2Cl_2, 20 °C): 212.2 (t, J = 10.1 Hz, CO), 191.3 (t, J = 7.6 Hz, CO), 161.0 (s, py), 142.2 (s, py), 101.9 (s, py), 30.6 (t, J = 15.0 Hz, $CH(CH_3)_2$), 29.3 (t, J = 15.3 Hz, $CH(CH_3)_2$), 19.2 (s, $CH(CH_3)_2$), 19.1 (s, $CH(CH_3)_2$), 18.9 (s, $CH(CH_3)_2$), 17.7 (s, $CH(CH_3)_2$). ^{31}P{^{1}H} NMR (δ, CD_2Cl_2, 20 °C): 106.6. IR (ATR, cm^{-1}): 2023 (ν_{CO}), 1953 (ν_{CO}), 1922 (ν_{CO}).

[W(PNP-*t*Bu)(CO)$_3$Br]Br (3c). This complex was prepared analogously to **3a** with $W(CO)_6$ (2.0 g, 5.68 mmol) and PNP-*t*Bu (**1c**) (2.26 g, 5.69 mmol) as starting materials. Yield: 2.51 g (60%). Anal. Calcd for $C_{24}H_{41}Br_2N_3O_3P_2W$: C, 34.93; H, 5.01; N, 5.09. Found: C, 34.81; H, 5.02; N, 5.20. ^{1}H NMR (δ, CD_2Cl_2, 20 °C): 9.11 (s, 2H, N*H*), 7.74 (d, J = 7.8 Hz, 2H, py), 7.23 (t, J = 8.7 Hz, 1H, py), 1.70 (d, J = 8.2 Hz, 9H, C(C*H*$_3$)$_3$), 1.68 (d, J = 7.3 Hz, 9H, C(C*H*$_3$)$_3$), 1.54 (d, J = 7.5 Hz, 9H, C(C*H*$_3$)$_3$), 1.48 (d, J = 7.1 Hz, 9H, C(C*H*$_3$)$_3$).

^{13}C{^{1}H} NMR (δ, CDCl$_3$, 20 °C): 229.9 (t, J = 14.8 Hz, CO), 212.9 (t, J = 7.6 Hz, CO), 162.6 (t, J = 4.2 Hz, py), 153.3 (d, J = 5.8 Hz, py), 149.9 (s, py), 103.8 (s, py), 46.0 (t, J = 7.2 Hz, C(CH$_3$)$_3$), 44.6 (t, J = 7.2 Hz, C(CH$_3$)$_3$), 31.9 (s, C(CH$_3$)$_3$), 30.4 (s, C(CH$_3$)$_3$), 26.9 (s, C(CH$_3$)$_3$). ^{31}P{^{1}H} NMR (δ, CD$_2$Cl$_2$, 20 °C): 131.6. IR (ATR, cm^{-1}): 2019 (ν_{CO}), 1941 (ν_{CO}), 1909 (ν_{CO}).

[Mo(PNP-Ph)(CO)$_3$Br]Br (4a). This complex was prepared analogously to **3a** with Mo(CO)$_6$ (300 mg, 1.14 mmol) and PNP-Ph (**1a**; 570 mg, 1.20 mmol) as starting materials. Yield: 775 mg (83%). Anal. Calcd for $C_{32}H_{25}Br_2MoN_3O_3P_2$: C, 47.03; H, 3.08; N, 5.14. Found: C, 46.95; H, 3.12; N, 5.01. ^{1}H NMR (δ, acetone-d_6, 20 °C): 8.70 (s, 2H, NH), 7.59 (m, 5H, Ph), 7.47 (m, 5H, Ph), 7.16 (t, J = 7.2 Hz, 1H, py), 7.01 (m, 5H, Ph), 6.85 (m, 5H, Ph), 6.56 (d, J = 7.8 Hz, 2H, py). ^{31}P{^{1}H} NMR (δ, acetone-d_6, 20 °C): 125.3. IR (ATR, cm^{-1}): 2040 (ν_{CO}), 1975 (ν_{CO}), 1875 (ν_{CO}).

[Mo(PNP-*i*Pr)(CO)$_3$Br]Br (4b). This complex was prepared analogously to **3a** with Mo(CO)$_6$ (500 mg, 1.89 mmol) and PNP-*i*Pr (**1b**; 678 mg, 1.98 mmol) as starting materials. Yield: 965 mg (75%). Anal. Calcd for $C_{20}H_{33}Br_2MoN_3O_3P_2$: C, 35.26; H, 4.88; N, 6.17. Found: C, 35.13; H, 4.92; N, 6.20. ^{1}H NMR (δ, CDCl$_3$, 20 °C): 9.08 (s, 2H, NH), 7.24 (d, J = 9.9 Hz, 2H, py), 7.10 (t, J = 7.4 Hz, 1H, py), 3.55 (m, 2H, CH(CH$_3$)$_2$), 2.96 (m, 2H, CH(CH$_3$)$_2$). 1.44 (m, 24H, CH(CH$_3$)$_2$). ^{13}C{^{1}H} NMR (δ, CDCl$_3$, 20 °C): 234.6 (t, J = 7.2 Hz, CO), 218.3 (t, J = 11.5 Hz, CO), 175.1 (s, py), 175.0 (s, py), 160.0 (t, J = 4.9 Hz, py), 142.1 (s, py), 102.7 (s, py), 30.8 (d, J = 12.8 Hz, CH(CH$_3$)$_2$), 30.6 (d, J = 14.9 Hz, CH(CH$_3$)$_2$), 30.3 (d, J = 12.4 Hz, CH(CH$_3$)$_2$), 30.1 (d, J = 11.6 Hz, CH(CH$_3$)$_2$), 19.4 (s, CH(CH$_3$)$_2$), 19.3 (s, CH(CH$_3$)$_2$), 19.1 (s, CH(CH$_3$)$_2$), 18.1 (s, CH(CH$_3$)$_2$). ^{31}P{^{1}H} NMR (δ, CDCl$_3$, 20 °C): 126.7. IR (ATR, cm^{-1}): 2030 (ν_{CO}), 1967 (ν_{CO}), 1936 (ν_{CO}).

[W(PNP-Ph)(CO)$_3$] (5a). A solution of **3a** (200 mg, 0.22 mmol) in THF (15 mL) was stirred in the presence of NaHg (10%) (16 mg, 0.66 mmol) for 8 h at room temperature. The solvent was then removed under reduced pressure. The residue was redissolved in acetone (10 mL), and the solution was filtered through Celite. After removal of the solvent under reduced pressure, a yellow solid was obtained, which was washed twice with diethyl ether (10 mL) and dried under vacuum. Yield: 140 mg (85%). Anal. Calcd for $C_{32}H_{25}N_3O_3P_2W$: C, 51.57; H, 3.38; N, 5.64. Found: C, 51.63; H, 3.41; N, 5.50. ^{1}H NMR (δ, acetone-d_6, 20 °C): 7.64 (t, J = 8.6 Hz, 1H, py), 7.44 (bs, 8H, Ph), 7.30 (m, 12H, Ph), 6.43 (d, J = 7.6 Hz, 2H, py), 5.93 (d, J = 8.9 Hz, 2H, NH). ^{13}C{^{1}H} NMR (δ, acetone-d_6, 20 °C): 206.0 (t, J = 4.6 Hz, CO), 196.6 (t, J = 9.1 Hz, CO), 159.6 (d, J = 4.7 Hz, py), 159.3 (d, J = 5.5 Hz, py), 142.1 (s, py), 132.0 (s, Ph), 131.0 (d, J = 12.4 Hz, Ph), 129.1 (d, J = 11.5 Hz, Ph), 127.9 (d, J = 6.6 Hz, Ph), 102.0 (d, J = 10.7 Hz, py). ^{31}P{^{1}H} NMR (δ, acetone-d_6, 20 °C): 100.2 (s, J_{W-P} = 327 Hz). IR (ATR, cm^{-1}): 1955 (ν_{CO}), 1847 (ν_{CO}), 1759 (ν_{CO}).

[W(PNP-*i*Pr)(CO)$_3$] (5b). This complex was prepared analogously to **5a** with **3b** (500 mg, 0.65 mmol) and NaHg (45 mg, 1.95 mmol) as starting materials. Yield: 315 mg (80%). Anal. Calcd for $C_{20}H_{33}N_3O_3P_2W$: C, 39.43; H, 5.46; N, 6.90. Found: C, 39.51; H, 5.42; N, 6.84. ^{1}H NMR (δ, CD$_2$Cl$_2$, 20 °C): 7.15 (t, J = 8.2 Hz, 1H, py), 6.15 (d, J = 7.9 Hz, 2H, py), 5.50 (bs, 2H, NH), 2.40 (m, 4H, CH(CH$_3$)$_2$), 1.24 (m, 24H, CH(CH$_3$)$_2$). ^{13}C{^{1}H} NMR (δ, CD$_2$Cl$_2$, 20 °C): 221.1 (t, J = 2.0 Hz, CO), 210.6 (t, J = 7.1 Hz, CO), 162.5 (t, J = 8.5 Hz, py), 137.1 (s, py), 96.6 (t, J = 3.1 Hz, py), 32.60 (t, J = 12.8 Hz, CH(CH$_3$)$_2$), 18.5 (t, J = 1.7 Hz, CH(CH$_3$)$_2$), 18.1 (t, J = 2.9 Hz, CH(CH$_3$)$_2$). ^{31}P{^{1}H} NMR (δ, CD$_2$Cl$_2$, 20 °C): 128.5 (s, J_{W-P} = 315 Hz). IR (ATR, cm^{-1}): 1929 (ν_{CO}), 1805 (ν_{CO}), 1784 (ν_{CO}).

[W(PNP-*t*Bu)(CO)$_3$] (5c). This complex was prepared analogously to **5a** with **3c** (350 mg, 0.42 mmol) and NaHg (30 mg, 1.27 mmol) as starting materials. Yield: 215 mg (77%). Anal. Calcd for $C_{24}H_{41}N_3O_3P_2W$: C, 43.32; H, 6.21; N, 6.32. Found: C, 43.23; H, 6.42; N, 6.48. ^{1}H NMR (δ, CD$_2$Cl$_2$, 20 °C): 7.37 (bs, 2H, NH), 7.18 (t, J = 8.0 Hz, 1H, py), 6.29 (d, J = 7.5 Hz, 2H, py), 1.41 (t, J = 5.6 Hz, 36H, C(CH$_3$)$_3$). ^{13}C{^{1}H} NMR (δ, acetone-d_6, 20 °C): 224.7 (t, J = 6.4 Hz,CO), 219.4 (t, J = 7.0 Hz, CO), 162.6 (d, J = 6.7 Hz, py), 137.8 (s, py), 97.1 (s, py), 40.7 (t, J = 7.5 Hz, C(CH$_3$)$_3$), 25.8 (d, J = 7.3 Hz, C(CH$_3$)$_3$). ^{31}P{^{1}H} NMR (δ, CD$_2$Cl$_2$, 20 °C): 147.2 (s, J_{W-P} = 329 Hz). IR (ATR, cm^{-1}): 1914 (ν_{CO}), 1799 (ν_{CO}), 1759 (ν_{CO}).

Alternative Synthesis of [Mo(PNP-*i*Pr)(CO)$_3$] (2b). This complex was prepared analogously to **5a** with **4b** (88 mg, 0.13 mmol) and NaHg (9 mg, 0.39 mmol) as starting materials. Yield: 61 mg (90%). All spectral data for **2a** are identical with those of the authentic sample reported previously.[13]

[Mo(PNP-Ph)(CO)$_3$H]BF$_4$ (7a). To a solution of **2a** (200 mg, 0.30 mmol) in CH$_2$Cl$_2$ (10 mL) was added HBF$_4$ ((46 μL, 0.45 mmol, 54% solution in Et$_2$O) at room temperature. After the solution was stirred overnight, a pale yellow precipitate was formed, which was collected on a glass frit, washed with diethyl ether, and dried under vacuum. Yield: 193 mg (85%). Anal. Calcd for $C_{32}H_{26}BF_4MoN_3O_3P_2$: C, 51.57; H, 3.52; N, 5.64. Found: C, 51.66; H, 3.59; N, 5.70. ^{1}H NMR (δ, acetone-d_6, −60 °C): 9.25 (s, 2H, NH), 8.23 (m, 13H, Ph, py), 7.93 (m, 8H, Ph), 6.99 (d, J = 8.0 Hz, 2H, py), −3.78 (dd, $^2J_{HP}$ = 21.6 Hz, $^2J_{HP}$ = 48.5 Hz, 1H, MoH). ^{13}C{^{1}H} NMR (δ, CD$_2$Cl$_2$, 20 °C): 212.7 (t, J = 11.2 Hz, CO), 203.2 (t, J = 8.4 Hz, CO), 158.4 (d, J = 6.1 Hz, py), 158.1 (d, J = 8.3 Hz, py), 141.6 (s, py), 135.3 (s, py), 134.5 (d, J = 55.6 Hz, Ph), 131.8 (s, Ph), 130.7 (d, J = 13.7 Hz, Ph), 129.0 (d, J = 11.1 Hz, Ph), 102.2 (d, J = 8.3 Hz, py). ^{31}P{^{1}H} NMR (δ, acetone-d_6, −60 °C): 111.5 (d, $^2J_{PP}$ = 88.4 Hz), 97.8 (d, $^2J_{PP}$ = 88.4 Hz). IR (ATR, cm^{-1}): 2042 (ν_{CO}), 1940 (ν_{CO}), 1937 (ν_{CO}).

[Mo(PNP-*i*Pr)(CO)$_3$H]BF$_4$ (7b). This complex was prepared analogously to **7a** with **2b** (200 mg, 0.38 mmol) and HBF$_4$ (78 μL, 0.58 mmol) as starting materials. Yield: 200 mg (87%). Anal. Calcd for $C_{20}H_{34}BF_4MoN_3O_3P_2$: C, 39.43; H, 5.63; N, 6.90. Found: C, 39.53; H, 5.71; N, 6.99. ^{1}H NMR (δ, acetone-d_6, −60 °C): 8.86 (d, J = 41.2 Hz, 2H, NH), 8.00 (t, J = 8.2 Hz, 1H, py), 6.95 (d, J = 2.91 Hz, 1H, py), 6.92 (d, J = 2.91 Hz, 1H, py), 3.27 (m, 4H, CH(CH$_3$)$_2$), 1.83 (m, 24H, CH(CH$_3$)$_2$), −4.98 (dd, $^2J_{HP}$ = 36.7 Hz, $^2J_{HP}$ = 51.0 Hz, 1H, MoH). ^{13}C{^{1}H} NMR (δ, CD$_2$Cl$_2$, 20 °C): 212.3 (t, J = 11.3 Hz, CO), 205.8 (t, J = 9.0 Hz, CO), 159.8 (d, J = 3.9 Hz, py), 159.7 (d, J = 3.9 Hz, py), 141.5 (s, py), 100.5 (d, J = 7.5 Hz, py), 31.5 (d, J = 29.5 Hz, CH(CH$_3$)$_2$), 17.8 (d, J = 2.3 Hz, CH(CH$_3$)$_2$). ^{31}P{^{1}H} NMR (δ, acetone-d_6, −60 °C): 142.3 (d, $^2J_{PP}$ = 90.4 Hz), 121.4 (d, $^2J_{PP}$ = 90.4 Hz). IR (ATR, cm^{-1}): 2035 (ν_{CO}), 1923 (ν_{CO}), 1920 (ν_{CO}).

[Mo(PNP-*t*Bu)(CO)$_3$H]BF$_4$ (7c). This complex was prepared analogously to **7a** with **2c** (240 mg, 0.42 mmol) and HBF$_4$ (85 μL, 0.62 mmol) as starting materials. Yield: 243 mg (87%). Anal. Calcd for $C_{24}H_{42}BF_4MoN_3O_3P_2$: C, 43.33; H, 6.36; N, 6.32. Found: C, 43.43; H, 6.42; N, 6.28. ^{1}H NMR (δ, acetone-d_6, −60 °C): 8.06 (bs, 2H, NH), 7.62 (t, J = 8.3 Hz, 1H, py), 6.62 (d, J = 7.9 Hz, 2H, py), 1.82 (d, J = 5.8 Hz, 18H, C(CH$_3$)$_3$), 1.80 (d, J = 6.5 Hz, 18H, C(CH$_3$)$_3$), −4.34 (dd, $^2J_{HP}$ = 20.7 Hz, $^2J_{HP}$ = 47.8 Hz, 1H, MoH). ^{13}C{^{1}H} NMR (δ, acetone-d_6, 20 °C): 213.7 (t, J = 12.1 Hz, CO), 209.5 (t, J = 9.4 Hz, CO), 160 (d, J = 7.0 Hz, py), 141.8 (s, py), 137.9 (s, py), 101.5 (d, J = 6.5 Hz, py), 97.3 (s, py), 41.2 (d, J = 15.8 Hz, C(CH$_3$)$_3$), 24.8 (d, J = 7.1 Hz, C(CH$_3$)$_3$). ^{31}P{^{1}H} NMR (δ, acetone-d_6, −60 °C): 158.8 (d, $^2J_{PP}$ = 81.5 Hz), 142.8 (d, $^2J_{PP}$ = 81.5 Hz). IR (ATR, cm^{-1}): 2019 (ν_{CO}), 1937 (ν_{CO}), 1916 (ν_{CO}).

[Mo(PNP^{Me}-*i*Pr)(CO)$_3$H]BF$_4$ (7d). This complex was prepared analogously to **7a** with **2d** (67 mg, 0.11 mmol) and HBF$_4$ (23 μL, 0.17 mmol) as starting materials. Yield: 63 mg (90%). Anal. Calcd for $C_{22}H_{38}BF_4MoN_3O_3P_2$: C, 41.46; H, 6.01; N, 6.59. Found: C, 41.55; H, 6.12; N, 6.47. ^{1}H NMR (δ, acetone-d_6, −60 °C): 7.93 (t, J = 8.2 Hz, 1H, py), 6.65 (d, J = 8.2 Hz, 2H, py), 3.41 (s, 6H, N(CH$_3$)), 3.25 (m, 4H, CH(CH$_3$)$_2$), 1.24 (d, J = 7.00 Hz, 6H, CH(CH$_3$)$_2$), 1.22 (d, J = 7.80 Hz, 12H, CH(CH$_3$)$_2$), 1.16 (d, J = 7.00 Hz, 6H, CH(CH$_3$)$_2$), −5.49 (dd, $^2J_{HP}$ = 20.9 Hz, $^2J_{HP}$ = 49.3 Hz, 1H, MoH). ^{13}C{^{1}H} NMR (δ, CD$_2$Cl$_2$, 20 °C): 210.8 (t, J = 10.8 Hz, CO), 205.4 (t, J = 9.5 Hz, CO), 161 (t, J = 5.2 Hz, py), 141.9 (s, py), 100.7 (s, py), 35.3 (s, NCH$_3$), 32.3 (d, J = 24.9 Hz, CH(CH$_3$)$_2$), 19.3 (d, J = 7.6 Hz, CH(CH$_3$)$_2$), 17.9 (s, CH(CH$_3$)$_2$). ^{31}P{^{1}H} NMR (δ, acetone-d_6, −60 °C): 166.1 (d, $^2J_{PP}$ = 85.4 Hz), 147.7 (d, $^2J_{PP}$ = 85.4 Hz). IR (ATR, cm^{-1}): 2028 (ν_{CO}), 1928 (ν_{CO}), 1910 (ν_{CO}).

[W(PNP-Ph)(CO)$_3$H]BF$_4$ (8a). This complex was prepared analogously to **7a** with **5a** (210 mg, 0.28 mmol) and HBF$_4$ (58 μL, 0.42 mmol) as starting materials. Yield: 186 mg (80%). Anal. Calcd for $C_{32}H_{26}BF_4N_3O_3P_2W$: C, 46.13; H, 3.15; N, 5.04. Found: C, 46.23; H,

Table 2. Details for the Crystal Structure Determinations of Compounds 3a·CH_3OH, 4b, 2d, 5b·THF·$^1/_2C_6H_{14}$, 5c·THF, 7a, 7d·CH_2Cl_2, and 8a

	3a·CH_3OH	4b	2d	5b·THF·$^1/_2C_6H_{14}$
formula	$C_{33}H_{29}Br_2N_3O_4P_2W$	$C_{20}H_{33}Br_2MoN_3O_3P_2$	$C_{22}H_{37}MoN_3O_3P_2$	$C_{27}H_{48}N_3O_4P_2W$
fw	937.20	681.19	549.43	724.47
cryst size, mm	0.16 × 0.06 × 0.05	0.59 × 0.20 × 0.18	0.24 × 0.14 × 0.10	0.50 × 0.40 × 0.20
color, shape	orange prism	yellow plate	yellow prism	yellow plate
cryst syst	triclinic	monoclinic	orthorhombic	monoclinic
space group	$P\bar{1}$ (No. 2)	$C2/c$ (No. 15)	$Pnma$ (No. 62)	$P2_1/c$ (No. 14)
a, Å	10.1741(6)	29.6913(15)	18.6552(5)	10.1399(10)
b, Å	13.1580(7)	10.7919(5)	12.1772(3)	15.5053(18)
c, Å	14.1040(8)	16.7764(8)	10.9035(2)	20.036(2)
α, deg	99.456(3)	90	90	90
β, deg	95.412(3)	97.954(1)	90	94.485(5)
γ, deg	104.306(3)	90	90	90
V, Å^3	1786.63(17)	5323.9(4)	2476.93(10)	3140.5(6)
T, K	296(2)	173(2)	100(2)	100(2)
Z	2	8	4	4
ρ_{calcd}, g cm^{-3}	1.742	1.700	1.473	1.532
μ(Mo Kα), mm^{-1}	5.598	3.640	0.687	3.815
F(000)	908	2720	1144	1468
abs corr	multiscan, 0.77−0.56	multiscan, 0.50−0.32	multiscan, 0.93−0.83	multiscan, 0.75−0.46
θ range, deg	1.96−30.00	2.30−30.00	2.18−30.07	1.66−30.00
no. of rflns measd	46633	36362	20758	77629
R_{int}	0.060	0.022	0.033	0.042
no. of unique rflns	10399	7732	3770	9124
no. of rflns with $I > 2\sigma(I)$	7880	6562	3328	6686
no. of params/restraints	393/6	294/96	167/0	335/75
R1 ($I > 2\sigma(I)$)^a	0.0385	0.0273	0.0217	0.0398
R1 (all data)	0.0625	0.0351	0.0276	0.0689
wR2 ($I > 2\sigma(I)$)	0.0822	0.0693	0.0507	0.0805
wR2 (all data)	0.0884	0.0734	0.0534	0.0907
min/max diff Fourier peaks, e Å^{-3}	−1.39/1.56	−1.01/0.97	−0.32/0.43	−1.80/1.85
	5c·THF	7a	7d·CH_2Cl_2	8a
formula	$C_{28}H_{49}N_3O_4P_2W$	$C_{32}H_{26}BF_4MoN_3O_3P_2$	$C_{23}H_{40}BCl_2F_4MoN_3O_3P_2$	$C_{32}H_{26}BF_4N_3O_3P_2W$
fw	737.48	745.25	722.17	833.16
cryst size, mm	0.30 × 0.17 × 0.15	0.42 × 0.35 × 0.28	0.32 × 0.30 × 0.14	0.24 × 0.08 × 0.06
color, shape	yellow block	yellow block	yellow plate	yellow column
cryst syst	monoclinic	orthorhombic	monoclinic	orthorhombic
space group	$P2_1/n$ (No. 14)	$Pbca$ (No. 61)	$P2_1/n$ (No. 14)	$Pbca$ (No. 61)
a, Å	8.9480(2)	17.4696(5)	8.4324(3)	17.5150(4)
b, Å	16.2069(4)	15.5290(4)	23.4895(7)	15.5022(3)
c, Å	21.6874(5)	23.3940(6)	16.2384(5)	23.3387(5)
α, deg	90	90	90	90
β, deg	95.539(1)	90	104.815(2)	90
γ, deg	90	90	90	90
V, Å^3	3130.41(13)	6346.5(3)	3109.46(17)	6336.9(2)
T, K	100(2)	100(2)	100(2)	100(2)
Z	4	8	4	8
ρ_{calcd}, g cm^{-3}	1.565	1.560	1.543	1.747
μ(Mo Kα), mm^{-1}	3.828	0.576	0.751	3.809
F(000)	1496	3008	1480	3264
abs corr	multiscan, 0.60−0.51	multiscan, 0.85−0.78	multiscan, 0.75−0.63	multiscan, 0.75−0.56
θ range, deg	1.89−30.00	1.96−30.00	2.17−30.00	1.96−30.00
no. of rflns measd	59364	147535	52608	103531
R_{int}	0.023	0.030	0.030	0.032
no. of unique rflns	9120	9239	9052	9225
no. of rflns with $I > 2\sigma(I)$	8540	8380	8280	8120
no. of params/restraints	355/0	440/0	366/0	440/0
R1 ($I > 2\sigma(I)$)^a	0.0202	0.0252	0.0216	0.0200
R1 (all data)	0.0226	0.0302	0.0253	0.0260
wR2 ($I > 2\sigma(I)$)	0.0470	0.0595	0.0504	0.0385

dx.doi.org/10.1021/om400254k | Organometallics 2013, 32, 3042−3052

Table 2. continued

	5c·THF	7a	7d·CH_2Cl_2	8a
wR2 (all data)	0.0479	0.0636	0.0525	0.0406
min/max diff Fourier peaks, e Å^{-3}	−1.03/1.40	−0.71/0.50	−0.43/0.45	−0.87/0.74

[a]R1 = $\sum||F_o| - |F_c||/\sum|F_o|$; wR2 = $\{\sum[w(F_o^2 - F_c^2)^2]/\sum[w(F_o^2)^2]\}^{1/2}$.

3.12; N, 5.20. ^{1}H NMR (δ, acetone-d_6, −60 °C): 9.74 (bs, 2H, N*H*), 8.15 (s, 8H, Ph), 8.25 (t, J = 8.4 Hz, 1H, py), 8.15 (m, 8H, Ph), 7.94 (m, 12H, Ph), 7.04 (d, J = 8.0 Hz, 2H, py), −3.43 (dd, $^2J_{HP}$ = 22.4 Hz, $^2J_{HP}$ = 53.8 Hz 1H, W*H*). ^{13}C{^{1}H} NMR (δ, acetone-d$_6$, 20 °C): 205.9 (t, J = 9.7 Hz, *C*O), 196.6 (t, J = 8.7 Hz, *C*O), 159.5 (d, J = 5.9 Hz, py), 159.3 (d, J = 5.9 Hz, py), 142.1 (s, py), 132.0 (s, py), 130.9 (d, J = 13.0 Hz, Ph), 129.5 (d, J = 13.7 Hz, Ph), 129.1 (d, J = 12.1 Hz, Ph), 127.9 (d, J = 4.6 Hz, Ph), 102.0 (d, J = 9.4 Hz, py). ^{31}P{^{1}H} NMR (δ,acetone-d$_6$, −60 °C): 95.5 (d, $^2J_{PP}$ = 85.9 Hz), 84.8 (d, $^2J_{PP}$ = 85.9 Hz). IR (ATR, cm^{-1}): 2038 (ν_{CO}), 1963 (ν_{CO}), 1918 (ν_{CO}).

[W(PNP-*i*Pr)(CO)$_3$H]BF$_4$ (8b). This complex was prepared analogously to **8a** with **5b** (200 mg, 0.33 mmol) and HBF_4 (20 μL, 0.49 mmol) as starting materials. Yield: 207 mg (90%). Anal. Calcd for $C_{20}H_{34}BF_4N_3O_3P_2W$: C, 34.46; H, 4.92; N, 6.03. Found: C, 34.55; H, 5.02; N, 6.10. ^{1}H NMR (δ, CD_2Cl_2, 20 °C): 8.47 (bs, 2H, N*H*), 7.50 (t, J = 8.5 Hz, 1H, py), 6.67 (d, J = 7.7 Hz, 2H, py), 2.41 (m, 4H, C*H*(CH_3)$_2$), 1.30 (m, 28H, CH(C*H*$_3$)$_2$), −4.83 (dd, $^2J_{HP}$ = 23.3 Hz, $^2J_{HP}$ = 54.7 Hz, 1H, W*H*). ^{13}C{^{1}H} NMR (δ, CD_2Cl_2, 20 °C): 205.5 (t, J = 8.5 Hz, *C*O), 198.0 (t, J = 8.1 Hz, *C*O), 160.1 (d, J = 3.9 Hz, py), 141.6 (s, py), 100.4 (d, J = 6.4 Hz, py), 31.9 (d, J = 25.5 Hz, *C*H(CH_3)$_2$), 18.0 (d, J = 4.2 Hz, CH(*C*H$_3$)$_2$). ^{31}P{^{1}H} NMR (δ, CD_2Cl_2, 20 °C): 125.9 (d, $^2J_{PP}$ = 80.0 Hz), 108.6 (d, $^2J_{PP}$ = 80.0 Hz). IR (ATR, cm^{-1}): 2027 (ν_{CO}), 1910 (ν_{CO}), 1906 (ν_{CO}).

[W(PNP-*t*Bu)(CO)$_3$H]BF$_4$ (8c). This complex was prepared analogously to **8a** with **5c** (200 mg, 0.30 mmol) and HBF_4 (18 μL, 0.45 mmol) as starting materials. Yield: 207 mg (90%). Anal. Calcd for $C_{24}H_{42}BF_4N_3O_3P_2W$: C, 38.27; H, 5.62; N, 5.58. Found: C, 38.29; H, 5.52; N, 5.52. ^{1}H NMR (δ, acetone-d_6, 20 °C): 8.00 (bs, 2H, N*H*), 7.60 (t, J = 6.7 Hz, 1H, py), 6.75 (d, J = 8.3 Hz, 2H, py), 1.59 (s, 18H, C(C*H*$_3$)$_3$), 1.53 (s, 18H, C(C*H*$_3$)$_3$). −4.16 (dd, $^2J_{HP}$ = 37.8 Hz, $^2J_{HP}$ = 50.8 Hz, 1H, W*H*). ^{31}P{^{1}H} NMR (δ, CD_2Cl_2, 20 °C): 141.1 (d, $^2J_{PP}$ = 83.6 Hz), 126.8 (d, $^2J_{PP}$ = 83.6 Hz). IR (ATR, cm^{-1}): 2021 (ν_{CO}), 1934 (ν_{CO}), 1897 (ν_{CO}).

X-ray Structure Determination. Single crystals of the complexes **3a**, **4b**, **2d**, **5b**,**c**, **7a**,**d**, and **8a** suitable for X-ray diffraction were mainly obtained by the solvent/antisolvent liquid−liquid diffusion method at room temperature using CH_2Cl_2/diethyl ether (**4b**, **2d**, **7a**,**d**, **8a**) or THF/n-hexane (**5b**,**c**), while **3a** was crystallized from methanol at −20 °C. The crystals of **3a**, **5b**,**c**, and **7d** were solvates (**3a**·CH_3OH, **5b**·THF·$^1/_2$hexane, **5c**·THF, **7d**·CH_2Cl_2). X-ray diffraction data were collected at T = 100 K on a Bruker Kappa APEX-2 CCD area detector diffractometer using graphite-monochromated Mo Kα radiation (λ = 0.71073 Å) and φ- and ω-scan frames covering complete spheres of the reciprocal space with θ_{max} = 30°. Corrections for absorption and λ/2 effects were applied using the program SADABS.[29] After structure solution with the program SHELXS97 refinement on F^2 was carried out with the program SHELXL97.[30] Non-hydrogen atoms were refined anisotropically. Most hydrogen atoms were placed in calculated positions and thereafter treated as riding. Crystal data are reported in Table 2, and detailed structural data are given in CIF format in the Supporting Information. Variata are as follows. The solid-state structure of **3a** (**3a**·CH_3OH) contained methanol and eventually some water disordered in a large oval infinite channel along the a axis embodying also the free bromide anions. The contribution of this solvent to the structure factors was removed with the procedure SQUEEZE of the program PLATON.[31] This structure shows also a Br by CO and a complementary CO by Br substitution disorder (equatorial C32−O3 by Br1′ and axial Br1 by C32′ and O3′ in 86:14 proportion). The crystal structure of **5b** contains an ordered THF and a disordered *n*-hexane solvent molecule, the latter across a center of inversion; the solid is therefore **5b**·THF·$^1/_2C_6H_{14}$. The contribution of the *n*-hexane solvent molecule to the structure factors was removed with the procedure SQUEEZE of the program PLATON. **5b** has also an orientation-disordered isopropyl group. The hydride complexes **7a** and **8a** form an isostructural pair, [Mo/W(PNP-Ph)(CO)$_3$H]BF$_4$, space group *Pbca*, with very similar unit cell dimensions, bond lengths, and bond angles. Both structures show a disorder of the equatorial CO group (C32−O3) and the hydride H atom (H1), which appear in two approximately equivalent positions left and right of the plane bisecting the complexes perpendicular to the pyridine ring. Due to the very good quality of the diffraction data of both complexes and due to good separations of the respective atom positions, it was possible to refine the approximately half-occupied positions of the hydride H atoms without restraints. The left/right ratio of the population parameter of CO and H in the molybdenum complex **7a** is 0.540(3)/0.460(3) and in the tungsten complex **8a** is 0.586(4)/0.414(4) (for C32, O3, H1/C32′, O3′, H1′; cf. Figures 7 and 9, which depict only the dominant nonprimed part). In contrast, the analogous molybdenum hydrido carbonyl complex **7d**·CH_2Cl_2 was perfectly ordered and gave on refinement with high-quality diffraction data a hydride position in very good agreement with complexes **7a** and **8a**, fully supporting the split atom refinements of these two crystal structures.

Computational Details. All calculations were performed using the GAUSSIAN 09 software package[32] on the Phoenix Linux Cluster of the Vienna University of Technology and the B3LYP functional[33] without symmetry constraints. The optimized geometries were obtained with the Stuttgart/Dresden ECP (SDD) basis set[34] to describe the electrons of the tungsten and molybdenum atoms. For all other atoms a standard 6-31g** basis set was employed.[35] All geometries were optimized without symmetry constraints. Frequency calculations were performed to confirm the nature of the stationary points, yielding one imaginary frequency for the transition states and none for the minima. Each transition state was further confirmed by following its vibrational mode downhill on both sides and obtaining the minima presented on the energy profiles. All energies reported are Gibbs free energies and thus contain zero-point, thermal, and entropy effects at 298 K and 1 atm pressure. A natural population analysis (NPA)[36] and the resulting Wiberg indices[27] were used to study the electronic structure and bonding of the optimized species. The NPA analysis was performed with the NBO 5.0 program.[37]

■ ASSOCIATED CONTENT

Supporting Information

CIF files giving complete crystallographic data and technical details for complexes **3a**, **4b**, **2d**, **5b**,**c**, **7a**,**d**, and **8a**. This material is available free of charge via the Internet at http://pubs.acs.org.

■ AUTHOR INFORMATION

Corresponding Author

*E-mail for K.K.: kkirch@mail.tuwien.ac.at.

Notes

The authors declare no competing financial interest.

■ ACKNOWLEDGMENTS

Financial support by the Austrian Science Fund (FWF) (Project No. P24202-N17) and by Fundação para a Ciência e Tecnologia, FCT (PEst-OE/QUI/UI0100/2011), is gratefully acknowledged

REFERENCES

(1) Dahloff, W. V.; Nelson, S. M. *J. Chem. Soc. A* **1971**, 2184.

(2) (a) Vasapollo, G.; Giannoccaro, P.; Nobile, C. F.; Sacco, A. *Inorg. Chim. Acta* **1981**, *48*, 125. (b) Steffey, B. D.; Miedaner, A.; Maciejewski-Farmer, M. L.; Bernatis, P. R.; Herring, A. M.; Allured, V. S.; Carperos, V.; DuBois, D. L. *Organometallics* **1994**, *13*, 4844. (c) Hahn, C.; Sieler, J.; Taube, R. *Chem. Ber.* **1997**, *130*, 939. (d) Hahn, C.; Vitagliano, A.; Giordano, F.; Taube, R. *Organometallics* **1998**, *17*, 2060. (e) Hahn, C.; Spiegler, M.; Herdtweck, E.; Taube, R. *Eur. J. Inorg. Chem.* **1999**, 435.

(3) Jiang, Q.; Van Plew, D.; Murtuza, S.; Zhang, X. *Tetrahedron Lett.* **1996**, *37*, 797.

(4) (a) Andreocci, M. V.; Mattogno, G.; Zanoni, R.; Giannoccaro, P.; Vasapollo, G. *Inorg. Chim. Acta* **1982**, *63*, 225. (b) Sacco, A.; Vasapollo, G.; Nobile, C.; Piergiovanni, A.; Pellinghelli, M. A.; Lanfranchi, M. *J. Organomet. Chem.* **1988**, *356*, 397. (c) Abbenhuis, R. A. T. M.; del Rio, I.; Bergshoef, M. M.; Boersma, J.; Veldman, N.; Spek, A. L.; van Koten, G. *Inorg. Chem.* **1998**, *37*, 1749.

(5) (a) Rahmouni, N.; Osborn, J. A.; De Cian, A.; Fisher, J.; Ezzamarty, A. *Organometallics* **1998**, *17*, 2470. (b) Sablong, R.; Newton, C.; Dierkes, P.; Osborn, J. A. *Tetrahedron Lett.* **1996**, *37*, 4933. (c) Sablong, R.; Osborn, J. A. *Tetrahedron Lett.* **1996**, *37*, 4937. (d) Barloy, L.; Ku, S. Y.; Osborn, J. A.; De Cian, A.; Fischer, J. *Polyhedron* **1997**, *16*, 291.

(6) (a) Zhang, J.; Leitus, G.; Ben-David, Y.; Milstein, D. *J. Am. Chem. Soc.* **2005**, *127*, 10840. (b) Zhang, J.; Gandelman, M.; Shimon, L. J. W.; Rozenberg, H.; Milstein, D. *Organometallics* **2004**, *23*, 4026. (c) Hermann, D.; Gandelman, M.; Rozenberg, H.; Shimon, L. J. W.; Milstein, D. *Organometallics* **2002**, *21*, 812.

(7) Gibson, D. H.; Pariya, C.; Mashuta, M. S. *Organometallics* **2004**, *23*, 2510.

(8) Katayama, H.; Wada, C.; Taniguchi, K.; Ozawa, F. *Organometallics* **2002**, *21*, 3285.

(9) Jia, G.; Lee, H. M.; Williams, I. D.; Lau, C. P.; Chen, Y. *Organometallics* **1997**, *16*, 3941.

(10) Müller, G.; Klinga, M.; Leskelä, M.; Rieger, B. *Z. Anorg. Allg. Chem.* **2002**, *628*, 2839.

(11) Ansell, J.; Wills, M. *Chem. Soc. Rev.* **2002**, *31*, 259.

(12) (a) Schirmer, W.; Flörke, U.; Haupt, H.-J. *Z. Anorg. Allg. Chem.* **1987**, *545*, 83. (b) Schirmer, W.; Flörke, U.; Haupt, H.-J. *Z. Anorg. Allg. Chem.* **1989**, *574*, 239.

(13) Benito-Garagorri, D.; Becker, E.; Wiedermann, J.; Lackner, W.; Pollak, M.; Mereiter, K.; Kisala, J.; Kirchner, K. *Organometallics* **2006**, *25*, 1900.

(14) (a) Benito-Garagorri, D.; Puchberger, M.; Mereiter, K.; Kirchner, K. *Angew. Chem., Int. Ed.* **2008**, *47*, 9142; *Angew. Chem.* **2008**, *120*, 9282. (b) Benito-Garagorri, D.; Alves, L. G.; Puchberger, M.; Mereiter, K.; Veiros, L. F.; Calhorda, M. J.; Carvalho, M. D.; Ferreira, L. P.; Godinho, M.; Kirchner, K. *Organometallics* **2009**, *28*, 6902. (c) Benito-Garagorri, D.; Alves, L. G.; Veiros, L. F.; Standfest-Hauser, C. M.; Tanaka, S.; Mereiter, K.; Kirchner, K. *Organometallics* **2010**, *29*, 4923.

(15) (a) Alves, L. G.; Dazinger, G.; Veiros, L. F.; Kirchner, K. *Eur. J. Inorg. Chem.* **2010**, 3160. (b) Benito-Garagorri, D.; Wiedermann, J.; Pollak, M.; Mereiter, K.; Kirchner, K. *Organometallics* **2007**, *26*, 217.

(16) Benito-Garagorri, D.; Mereiter, K.; Kirchner, K. *Eur. J. Inorg. Chem.* **2006**, 4374.

(17) Lang, H.-F.; Fanwick, P. E.; Walton, R. A. *Inorg. Chim. Acta* **2002**, *392*, 1.

(18) (a) Kinoshita, E.; Arashiba, K.; Kuriyama, S.; Miyake, Y.; Shimazaki, R.; Nakanishi, H.; Nishibayashi, Y. *Organometallics* **2012**, *31*, 8437. (b) Arashiba, A.; Sasaki, K.; Kuriyama, S.; Miyake, Y.; Nakanishi, H.; Nishibayashi, Y. *Organometallics* **2012**, *31*, 2035. (c) Arashiba, K.; Miyake, Y.; Nishibayashi, Y. *Nat. Chemistry* **2011**, *3*, 120.

(19) Wingard, L. A.; White, P. S.; Templeton, J. L. *Dalton Trans.* **2012**, *41*, 11438.

(20) For examples of molybdenum and tungsten hydridocarbonyl complexes, see: (a) Burchell, R. P. L.; Sirsch, P.; Decken, A.; McGrady, G. S. *Dalton Trans.* **2009**, 5851. (b) Namorado, S.; Cui, J.; de Azevedo, C. G.; Lemos, M. A.; Duarte, M. T.; Ascenso, J. R.; Dias, A. R.; Martins, A. M. *Eur. J. Inorg. Chem.* **2007**, 1103. (c) Shafiq, F.; Szaldza, D. J.; Creutz, C.; Bullock, R. M. *Organometallics* **2000**, *19*, 824. (d) Calvo, M.; Gomez-Sal, P.; Manzanero, A.; Royo, P. *Polyhedron* **1998**, *17*, 1081. (e) Brammer, L.; Zhao, D.; Bullock, R. M.; McMullan, R. K. *Inorg. Chem.* **1993**, *32*, 4819. (f) Protasiewicz, J. D.; Theopold, K. H. *J. Am. Chem. Soc.* **1993**, *115*, 5559. (g) Caffyn, A. J. M.; Feng, S. G.; Dierdorf, A.; Gamble, A. S.; Eldredge, P. A.; Vossen, M. R.; White, P. S.; Templeton, J. L. *Organometallics* **1991**, *10*, 2842.

(21) (a) Cotton, A. F.; Falvello, L. R.; Meadows, J. H. *Inorg. Chem.* **1984**, *24*, 514. (b) Boyden, J. A.; Colton, R. *Aust. J. Chem.* **1968**, *21*, 2567.

(22) For pincers with non-meridional coordination geometries see: Adams, J. J.; Arulsamy, N.; Roddick, D. M. *Organometallics* **2011**, *30*, 697.

(23) Curtis, M. D.; Shiu, K.-B. *Inorg. Chem.* **1985**, *24*, 1213.

(24) Baker, P. K.; Al-Jahdali, M.; Meehan, M. M. *J. Organomet. Chem.* **2002**, *648*, 99. (b) Baker, P. K.; Drew, M. G. B.; Moore, D. S. *J. Organomet. Chem.* **2002**, *663*, 45.

(25) (a) Hoffmann, R.; Beier, B. F.; Muetterties, E. L.; Rossi, A. R. *Inorg. Chem.* **1977**, *16*, 511. (b) Thompson, H. B.; Bartell, L. S. *Inorg. Chem.* **1968**, *7*, 488.

(26) Parr, R. G.; Yang, W. In *Density Functional Theory of Atoms and Molecules*; Oxford University Press: New York, 1989.

(27) (a) Wiberg, K. B. *Tetrahedron* **1968**, *24*, 1083. (b) Wiberg indices are electronic parameters related to the electron density between atoms. They can be obtained from a natural population analysis and provide an indication of the bond strength.

(28) Perrin, D. D.; Armarego, W. L. F. *Purification of Laboratory Chemicals*, 3rd ed.; Pergamon: New York, 1988.

(29) Bruker programs: *APEX2, version 2009.9-0*; *SAINT, version 7.68 A*; *SADABS, version 2008/1*; *SHELXTL, version 2008/4*, Bruker AXS Inc., Madison, WI, 2009.

(30) Sheldrick, G. M. *Acta Crystallogr.* **2008**, *A64*, 112−122.

(31) Spek, A. L. *J. Appl. Crystallogr.* **2003**, *36*, 7−13.

(32) Frisch, M. J. et al.. *Gaussian 09, Revision A.02*; Gaussian, Inc., Wallingford, CT, 2009.

(33) (a) Becke, A. D. *J. Chem. Phys.* **1993**, *98*, 5648. (b) Miehlich, B.; Savin, A.; Stoll, H.; Preuss, H. *Chem. Phys. Lett.* **1989**, *157*, 200. (c) Lee, C.; Yang, W.; Parr, G. *Phys. Rev. B* **1988**, *37*, 785.

(34) (a) Haeusermann, U.; Dolg, M.; Stoll, H.; Preuss, H. *Mol. Phys.* **1993**, *78*, 1211. (b) Kuechle, W.; Dolg, M.; Stoll, H.; Preuss, H. *J. Chem. Phys.* **1994**, *100*, 7535. (c) Leininger, T.; Nicklass, A.; Stoll, H.; Dolg, M.; Schwerdtfeger, P. *J. Chem. Phys.* **1996**, *105*, 1052.

(35) (a) McLean, A. D.; Chandler, G. S. *J. Chem. Phys.* **1980**, *72*, 5639. (b) Krishnan, R.; Binkley, J. S.; Seeger, R.; Pople, J. A. *J. Chem. Phys.* **1980**, *72*, 650. (c) Wachters, A. J. H. *Chem. Phys.* **1970**, *52*, 1033. (d) Hay, P. J. *J. Chem. Phys.* **1977**, *66*, 4377. (e) Raghavachari, K.; Trucks, G. W. *J. Chem. Phys.* **1989**, *91*, 1062. (f) Binning, R. C., Jr.; Curtiss, L. A. *J. Comput. Chem.* **1990**, *11*, 1206. (g) McGrath, M. P.; Radom, L. *J. Chem. Phys.* **1991**, *94*, 511.

(36) (a) Carpenter, J. E.; Weinhold, F. *J. Mol. Struct. (THEOCHEM)* **1988**, *169*, 41. (b) Carpenter, J. E. Ph.D. Thesis, University of Wisconsin, Madison, WI, 1987. (c) Foster, J. P.; Weinhold, F. *J. Am. Chem. Soc.* **1980**, *102*, 7211. (d) Reed, A. E.; Weinhold, F. *J. Chem. Phys.* **1983**, *78*, 4066. (e) Reed, A. E.; Weinhold, F. *J. Chem. Phys.* **1985**, *83*, 1736. (f) Reed, A. E.; Weinstock, R. B.; Weinhold, F. *J. Chem. Phys.* **1985**, *83*, 735. (g) Reed, A. E.; Curtiss, L. A.; Weinhold, F. *Chem. Rev.* **1988**, *88*, 899−926. (h) Weinhold, F.; Carpenter, J. E. *The Structure of Small Molecules and Ions*; Plenum: New York, 1988; p 227.

(37) Glendening, E. D.; Badenhoop, J. K.; Reed, A. E.; Carpenter, J. E.; Bohmann, J. A.; Morales, C. M.; Weinhold, F. *NBO 5.0*; Theoretical Chemistry Institute, University of Wisconsin, Madison, WI, 2001.